

FIG. 3. GO analysis of PC12 proteins differentially expressed after NGF stimulation. A, work flow for proteomics GO analysis (MANGO method). MANGO (a Web application), composed of the MySQL 4.0 and scripts written in Java, automatically executed the following steps. First, 1,482 proteins with multiple species matches were converted to human orthologs according to the conversion steps using Ensembl Mart files shown in the figure. Then the converted human orthologs were annotated with GO according to the UniProt GOA data set (described under "Experimental Procedures"). The resulting list of 1,404 GO-annotated human proteins was used as the PC12PRS as shown in supplemental Table 4. GeneSpring GX was used to determine statistically overrepresented GO categories from the iTRAQ data set. B, classification by annotated biological processes of the PC12PRS (a), 39 up-regulated (b), and 33 down-regulated (c) proteins identified with the iTRAQ method.

tained at 37 °C under the air condition of 5% CO₂ in the chamber set under the camera during the observation. Images were obtained by using a 20× UPlan SApo objective (Olympus IX81). The camera, shutters, and filter wheel were controlled by MetaMorph imaging software (Molecular Devices), and the images were collected every 10 min with an exposure time of 50 ms.

RESULTS

Identification of Differentially Expressed Proteins in Response to NGF in PC12 Cells—For the fourplex iTRAQ labeling, four independent, separately cultured cell lysates were prepared in parallel. The tryptic peptides from untreated cells were labeled with mass 114 and 115 isobaric iTRAQ tags, and those from NGF-treated cells were labeled with mass 116 and 117 isobaric iTRAQ tags. The iTRAQ-labeled peptides were then fractionated by cation exchange column chromatography and analyzed with LC-MS/MS using both MALDI and ESI (Fig. 1).

With LC-MALDI-MS/MS, 1,324 proteins were identified from 14,710 peptide sequences; in contrast, with LC-ESI-MS/MS, 902 proteins were identified from 12,769 peptide sequences. Only 744 proteins were identified by both systems, and 580 and 158 proteins were uniquely identified with LC-MALDI-MS/MS and LC-ESI-MS/MS, respectively. In total, 1,482 proteins were identified with >95% confidence (Fig. 2A and supplemental Table 1). At a -fold change of >20% (ratio >1.20 or <0.83), 15 proteins identified with LC-MALDI-MS/MS were up-regulated, and 19 were down-regulated, whereas 32 identified with LC-ESI-MS/MS were up-regulated, and 18 were down-regulated (p value <0.05) (Fig. 2, B and C). Eight up- and four down-regulated proteins were identified by both systems, and seven or 24 up- and 15 or 14 down-regulated proteins were uniquely identified with LC-MALDI-MS/MS or LC-ESI-MS/MS, respectively (Fig. 2, B and C). In total, 72 proteins (39 up- and 33 down-regulated) were differentially expressed in response to NGF. Among the NGF-responsive proteins, 64 were newly identified in this study (Table I and supplemental Tables 2 and 3).

Proteomics GO Analysis of NGF-responsive Proteins—The list of differentially expressed proteins was prepared for use in GO analysis with GeneSpring using a new, in-house taxonomy conversion/GO annotation tool, MANGO (a Web application) (Fig. 3A). First the taxonomies of all 1,482 identified proteins (multiple species matches) were converted to the *Homo sapiens* taxonomy. 1,404 of them were assigned human orthologs and annotated with GO information from UniProt. This GO-annotated list, compiled using the MANGO tool, was designated as the PC12 proteome reference set (PC12PRS) on which two distinct proteomics GO analyses were subsequently performed (supplemental Table 4). In the

first analysis, to determine the overrepresented biological processes specifically related to the NGF-induced PC12 cell differentiation, we simply compared the GO categories represented by the differentially expressed proteins in the PC12PRS with the GO categories represented by the PC12PRS overall (Fig. 3B). From this we found that the following biological processes occurred significantly more frequently in the GO annotations of the 39 up-regulated proteins than they did in the PC12PRS as a whole: “developmental process” (14 *versus* 6%), “multicellular organismal process” (10 *versus* 5%), and “response to stimulus” (8 *versus* 4%) (Fig. 3B, a and b). Also on the other hand, the occurrence ratio of “metabolic process” (30 *versus* 23%) was higher in the GO annotations of the 33 down-regulated proteins than in those of the PC12PRS as a whole (Fig. 3B, a and c). Next to obtain further statistical interpretation, a second proteomics GO analysis of the differentially expressed proteins in the PC12PRS (supplemental Table 4) was performed to determine which biological processes were enriched in the 39 up-regulated and the 33 down-regulated proteins (Table II). Using these data, a GO tree view was built to clarify the interrelationships of these biological processes (Fig. 3C). The part of the tree comprising the up-regulated proteins was mainly divided into six branches, which included “cell morphogenesis” (p value = 0.000518), “apoptosis (cell survival)” (p value = 0.0377), “homeostatic process” (p value = 0.0162), “cell motility” (p value = 0.000118), “response to stress” (p value = 0.000118), and “cell differentiation” (p value = 0.00372) (Tables II and III and Fig. 3C). On the other hand, the part of the tree comprising the down-regulated proteins included cellular metabolic processes, especially RNA and DNA metabolic processes (Tables II and III).

Biological Validation of Newly Identified NGF-responsive Proteins Related to GO Categories Extracted by MANGO—Of the six up-regulated groups listed in Table II, we focused on cell morphogenesis and apoptosis/cell survival (Fig. 3C and Table III) and used a time course analysis by Western blotting to study the expression patterns of the up-regulated proteins related to these processes (Fig. 4). Neurosecretory protein VGF, the most significantly up-regulated protein identified by both LC-MALDI-MS/MS and LC-ESI-MS/MS (Table I and supplemental Fig. 1), was used as a positive control of the time-dependently increased protein by Western blotting (Fig. 4). Seven proteins, CRMP-4, MAGED1, PAIRBP1, protein-disulfide isomerase, peroxiredoxin 6, ProT α , and TCTP, were up-regulated in response to NGF with different expression patterns in the time course study (Fig. 4, A and B, and supplemental Fig. 2). Interestingly TCTP and MAGED1 expression

C, a GO hierarchy tree of biological processes annotating the 39 up-regulated proteins. GO analysis was performed by using GeneSpring GX software. A GO tree view composed of enriched biological processes in the up-regulated proteins was built according to the tree view in AmiGO. Direct and indirect hierarchies are indicated by *full* and *dotted lines with arrows*, respectively. The number of molecules and p values (p Val) for biological processes annotated are shown in the tree.

Proteomics Analysis of PC12 Cell Differentiation

TABLE II
Overrepresented biological processes by proteomics GO analysis of proteins differentially expressed in response to NGF stimulation

Categories	All proteins in category	Percentage of all proteins in category	Up- or down-regulated proteins in category	Percentage of up- or down-regulated proteins in category	p value
Up-regulated proteins					
GO:8150: biological process	1,245	100	34	100	1
GO:32502: developmental process	231	18.55	18	52.94	4.82e-06
GO:48856: anatomical structure development	126	10.12	14	41.18	1.41e-06
GO:32501: multicellular organismal process	186	14.94	13	38.24	0.000635
GO:48731: system development	99	7.952	12	35.29	4.18e-06
GO:7275: multicellular organismal development	125	10.04	12	35.29	5.02e-05
GO:6950: response to stress	95	7.631	10	29.41	0.000118
GO:48869: cellular developmental process	145	11.65	10	29.41	0.00372
GO:30154: cell differentiation	145	11.65	10	29.41	0.00372
GO:50896: response to stimulus	163	13.09	10	29.41	0.00878
GO:48468: cell development	121	9.719	9	26.47	0.0037
GO:9653: anatomical structure morphogenesis	63	5.06	7	20.59	0.00111
GO:32989: cellular structure morphogenesis	40	3.213	6	17.65	0.000518
GO:902: cell morphogenesis	40	3.213	6	17.65	0.000518
GO:7399: nervous system development	48	3.855	6	17.65	0.00141
GO:65008: regulation of biological quality	56	4.498	6	17.65	0.00319
GO:48513: organ development	60	4.819	6	17.65	0.00455
GO:48518: positive regulation of biological process	93	7.47	6	17.65	0.036
GO:6915: apoptosis	94	7.55	6	17.65	0.0377
GO:12501: programmed cell death	95	7.631	6	17.65	0.0394
GO:8219: cell death	99	7.952	6	17.65	0.047
GO:48523: negative regulation of cellular process	99	7.952	6	17.65	0.047
GO:16265: death	99	7.952	6	17.65	0.047
GO:6457: protein folding	72	5.783	5	14.71	0.042
GO:30030: cell projection organization and biogenesis	18	1.446	4	11.76	0.00108
GO:48858: cell projection morphogenesis	18	1.446	4	11.76	0.00108
GO:32990: cell part morphogenesis	18	1.446	4	11.76	0.00108
GO:19725: cell homeostasis	36	2.892	4	11.76	0.0147
GO:42592: homeostatic process	37	2.972	4	11.76	0.0162
GO:6928: cell motility	50	4.016	4	11.76	0.0439
GO:51674: localization of cell	50	4.016	4	11.76	0.0439
GO:31175: neurite development	13	1.044	3	8.824	0.00442
GO:48666: neuron development	14	1.124	3	8.824	0.00552
GO:30003: cation homeostasis	17	1.365	3	8.824	0.00975
GO:30182: neuron differentiation	17	1.365	3	8.824	0.00975
GO:6873: cell ion homeostasis	18	1.446	3	8.824	0.0115
GO:30001: metal ion transport	18	1.446	3	8.824	0.0115
GO:50801: ion homeostasis	18	1.446	3	8.824	0.0115
GO:22008: neurogenesis	19	1.526	3	8.824	0.0134
GO:48699: generation of neurons	19	1.526	3	8.824	0.0134
GO:48878: chemical homeostasis	19	1.526	3	8.824	0.0134
GO:8284: positive regulation of cell proliferation	20	1.606	3	8.824	0.0154
GO:9966: regulation of signal transduction	29	2.329	3	8.824	0.0419
GO:42127: regulation of cell proliferation	29	2.329	3	8.824	0.0419
GO:7243: protein kinase cascade	30	2.41	3	8.824	0.0457
GO:9611: response to wounding	30	2.41	3	8.824	0.0457
Down-regulated proteins					
GO:8150: biological process	1,245	100	29	100	1
GO:44237: cellular metabolic process	824	66.18	24	82.76	0.0386
GO:43283: biopolymer metabolic process	389	31.24	15	51.72	0.0161
GO:61 nucleobase, nucleoside, nucleotide, and nucleic acid	337	27.07	14	48.28	0.011
GO:6397: mRNA processing	86	6.908	7	24.14	0.00263
GO:16071: mRNA metabolic process	101	8.112	7	24.14	0.0066
GO:6396: RNA processing	107	8.594	7	24.14	0.00907
GO:8380: RNA splicing	86	6.908	6	20.69	0.0119
GO:6259: DNA metabolic process	70	5.622	5	17.24	0.0201
GO:6281: DNA repair	23	1.847	3	10.34	0.0147
GO:6974: response to DNA damage stimulus	25	2.008	3	10.34	0.0185
GO:9719: response to endogenous stimulus	27	2.169	3	10.34	0.0228

TABLE III
The differentially expressed proteins related to the enriched biological processes

GO categories	Protein name (abbreviation) ^a
Up-regulated proteins	
Cell differentiation	SQSTM, RAC1, MAP1B, ENPL, CROP, NEUM, GAL1, TCTP, SCG2, S100A6, PROTA, ^b PAIRBP1 ^b
Response to stress	RAC1, SQSTM, ENPL, DNJA1, CROP, AT1A1, SCG2, ANXA2, OXRP, PRDX6
Cell morphogenesis	RAC1, RADI, S100A6, ENOA, NEUM, MAP1B, MAGED1, ^b CRMP4 ^b
Apoptosis (cell survival)	SQSTM, ENPL, TCTP, CROP, LEG1, SCG2, PAIRBP1, ^b MAGED1, ^b PROTA ^b
Homeostatic process	ENPL, AT1A1, PDI, TCTP,
Cell motility	MOES, AT1A1, SGTA, RAC1
Down-regulated proteins	
DNA and RNA metabolic process	HNRL, SRR35, LSM8, FUBP2, HNRPF, SFRS2, PRP19, PCNA, H2B1C, H2B2A, FEN1
Other cellular metabolic process	VTDB, TBB4, GALK1, RL34, UBP48, CSK21, RLA0, IDHP, TIM13, PRPS2, DDC, RL6, APT

^a The abbreviation of the protein name listed in Table I are shown in this table.

^b These proteins were not annotated with the enriched biological processes, but they are speculated to be related to the biological process as reported in Refs. 34 and 35 for PAIRBP1, in Ref. 37 for PROTA, in Ref. 38 for MAGED1, and in Ref. 55 for CRMP4.

increased for 12 h and then gradually decreased. On the other hand, galectin-1 and ProT α expression levels peaked at 48 and 24 h, respectively. CRMP-4 and PAIRBP1 expression levels were constantly up-regulated during 12–72 h of NGF stimulation. The down-regulated protein, PCNA, was also consistently regulated in response to NGF (Fig. 4A). PAIRBP1 (34, 35), TCTP (36), ProT α (37), and MAGED1 (38) have been speculated to be functionally related to cellular differentiation and survival/apoptosis. We therefore sought to identify the roles of these proteins. Immunocytochemistry (ICC) showed that PAIRBP1 was expressed not only in the cytoplasm but also in the neurites, especially at the tips and junctions (Fig. 5A, *g* and *i*, arrowheads), whereas MAGED1 was expressed only in the cytoplasm (Fig. 5D, *g* and *i*). TCTP and ProT α were strongly expressed in the nucleus in response to NGF (Fig. 5, *B* and *C*, *g* and *i*, arrows). These results suggested that those proteins were involved in NGF-treated cellular responses.

Suppression of Differentially Expressed Proteins by siRNA Treatment—PAIRBP1, TCTP, ProT α , and MAGED1 were further analyzed using specific siRNAs to investigate their functions. siRNA-induced down-regulation was confirmed by Western blotting and ICC using their specific antibodies (Fig. 6, *A* and *B*) followed by a test of whether or not their suppression morphologically influenced the PC12 neurite formation. As expected, significant inhibition of the neurite formation was observed (Fig. 6B). Interestingly the suppression of MAGED1 caused aggregation of differentiating cells (Fig. 6, *B*, *IV* and *C*, *a*, and supplemental Movie 5). Furthermore we calculated the number and total length of neurites in differentiating cells and found that these measurements were certainly decreased by the suppression of each protein (Fig. 6C, *b* and *c*). In addition, apoptotic phenotypes were observed in NGF-stimulated cells treated with PAIRBP1, TCTP, or ProT α siRNA (Fig. 6C, *a* and supplemental Movies 2–4). We therefore observed the effects of the down-regulation of these proteins by siRNA on the survival of NGF-treated PC12 cells using PI staining for apoptotic cells coupled with nuclear staining by Hoechst33342.

PAIRBP1, TCTP, or ProT α suppression caused a significant increase in PI-positive cells, whereas suppression of MAGED1 did not (Fig. 6C, *d* and *e*). These results suggested that, in PC12 cells, PAIRBP1, TCTP, ProT α , and MAGED1 regulate NGF-induced differentiation and that, except for MAGED1, they are involved in cell survival.

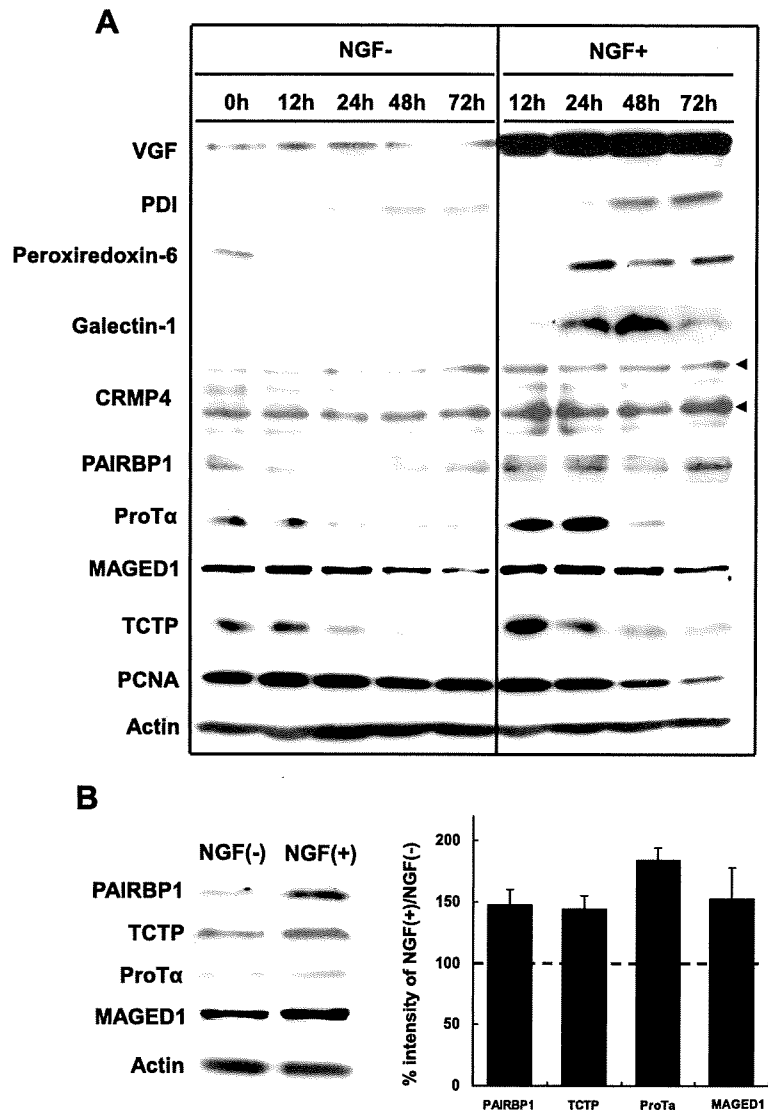
DISCUSSION

MS-based techniques targeting functional proteins in biological specimens have been developed to improve sensitivity, quantitation, and throughput. However, their application to biological study has not been satisfactory because their independent development has not met the needs of cell biologists and because of the lack of a sequential protocol and associated user-friendly analysis tools. Here we present a concise strategy consisting of sequential MS-based, *in silico*, and cell biological analyses to study the mechanisms of neuronal differentiation using PC12 cells.

Using MALDI-TOF-TOF and ESI-QqTOF in parallel, not only were certain proteins identified by both methods, but also unique proteins were independently identified by either of the methods. These data were combined to increase the number of identified proteins. It seemed important to know what kind of differences there were between the unique peptides identified by either of the systems. Previously Stapels and Barofsky (39) reported that the ESI system favored the identification of hydrophobic peptides whereas the MALDI system tended to lead to the identification of basic and aromatic peptides in the analysis of *E. coli* DNA-binding proteins. We noticed that the peptides identified by ESI-QqTOF had relatively higher theoretical pI values and molecular weights (pI = 6.46 and M_r = 1,694.4 on average) compared with those identified by MALDI-TOF-TOF (pI = 5.81 and M_r = 1,651.6 on average). The discrepancy, which seems contradictory, between our results and those of Stapels and Barofsky (39) may be explained by differences in sample, type of proteins analyzed, and the presence or absence of modification such as iTRAQ

Proteomics Analysis of PC12 Cell Differentiation

FIG. 4. Immunoblot images of PC12 proteins differentially expressed in response to NGF stimulation. Cell lysates were prepared at different time points as indicated. Actin expression was assessed for equal loading for all the proteins. **A**, the representative images are shown in four reproducible experiments. *Upper and lower arrowheads* show isoforms 1 and 2 of CRMP4, respectively. Some of those proteins showed a change in their expression levels even in untreated cells probably because of certain signals from collagen coated on the plates. **B**, Western blot images and quantification of the above four proteins PAIRBP1, TCTP, ProT α , and MAGED1 in NGF-stimulated PC12 cells. Cell lysates were prepared at 48 h after NGF stimulation. Actin expression was assessed for equal loading for all the proteins. The representative images are shown in four reproducible experiments. The ratios of percent intensities of the four proteins in NGF-stimulated versus untreated PC12 obtained from four separate identical experiments are shown in the histogram. *Error bars* represent S.D. The ratios were largely consistent with the corresponding iTRAQ ratios.

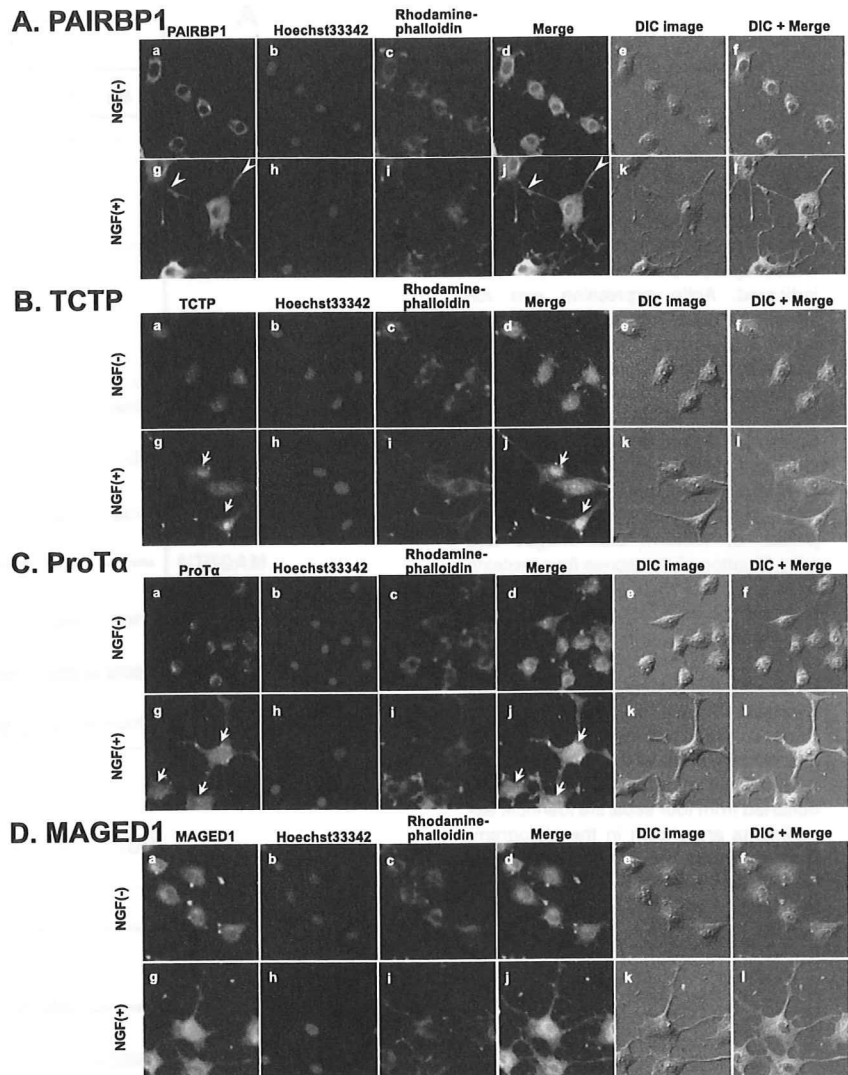


labeling. These results suggest that both MS systems may be complementary due to the biases of the two ionization systems and that analyses should be performed using both instruments to obtain more comprehensive information out of a given set of samples in a proteomics study.

In total, we analyzed 1,482 proteins with iTRAQ quantitation data of 4,899 proteins from 40,037 peptides identified by using the Mascot search engine (data not shown) in this study. To understand how our identification strategy covers the proteins expressed in PC12 cells, we analyzed the cellular component locations of all the identified proteins by the MANGO method and compared them with those of all human proteins listed in the Swiss-Prot database (20,332 entries, Release 57.2 of May 5, 2009) (supplemental Table 5). Of the 1,404 total identified human orthologs (PC12RPS), 1,231 were annotated

with cellular component data. Of the latter, 758 (62%), 166 (13%), and 118 (10%) proteins were annotated with "cytoplasm," "mitochondrion," and "plasma membrane," respectively. On the other hand, among 16,530 human proteins from the Swiss-Prot database annotated with cellular component data, 7,106 (43%), 1,033 (6%), and 3,632 (22%) proteins were annotated with cytoplasm, mitochondrion, and plasma membrane, respectively. In the PC12RPS, the occurrence ratios of cytoplasm (62%) and mitochondrion (13%) were higher than those in the Swiss-Prot human proteins (43 and 6%, respectively), whereas the ratio of plasma membrane (10%) in PC12RPS was lower than that in the Swiss-Prot human proteins (22%). By combining this ratio of plasma membrane with the ratio of "organelle membrane" proteins (10.97%), the percentage of membrane proteins in the total proteins identified

Fig. 5. Analysis of NGF-responsive proteins by ICC. PC12 cells were treated with NGF for 48 h. Cells were fixed and incubated with antibodies against the indicated proteins (A, PAIRBP1; B, TCTP; C, ProT α , and D, MAGED1) followed by detection with Alexa Fluor 488-labeled secondary antibodies (a and g) and observation with a fluorescence microscope. Nuclear and F-actin were stained with Hoechst33342 (b and h) and rhodamine-phalloidin (c and i), respectively. The merged images for a, b, c and g, h, i are shown in d and j, respectively. The merged images for d, e and j, k are shown in f and l. Differential interference contrast (DIC) images of PC12 cells in the same field are shown in e and k. Arrowheads indicate the PAIRBP1 expression in the neurite junctions and tips. Arrows indicate the TCTP and ProT α expression in the nucleus.



in our study becomes more than 20%. From these results, it is suggested that although cytoplasmic and mitochondrial proteins are largely favored in our method other components such as membrane and nuclear proteins can be also identified in significant numbers (supplemental Table 5).

From 1,482 proteins identified in iTRAQ quantitation, 72 differentially expressed proteins, including 39 up-regulated and 33 down-regulated, were extracted. The up-regulation of neurosecretory protein VGF (40), neuromodulin (41), chromogranin A (42), annexin A2 (43), peripherin (44), MAP1B (45), AHNAK (46), and secretogranin 2 (42) was observed as reported previously (Table II). Eighteen proteins in our results also corresponded to NGF-responsive genes in cDNA microarray data of Dijkmans *et al.* (23) (Table II) that coincided with our results, showing the confidence and reliability of our methods. Sixty-four proteins were hereto-

fore unreported (Table II). The majority were cytoskeletal organizing components, such as moesin, radixin, MAP1B, annexin A2, peripherin, CRMP-4, RAC1, keratin-8, and keratin-18, whose changes in expression suggested roles for them in the cytoskeletal reorganization for cellular motility and morphogenesis. Interestingly PCNA and flap endonuclease 1 are both required for DNA replication, and both histones H2A and H2B are nucleosome components, all of which were down-regulated by NGF treatment. These results suggested that the down-regulation of these proteins was a factor in the arrest of cell division and the initiation of PC12 neuronal differentiation.

Further biological and functional interpretation of the above proteins was performed by proteomics GO analysis using the GO annotation and analysis tool. Here we encountered two problems. First, unlike microarray data, proteomics data con-

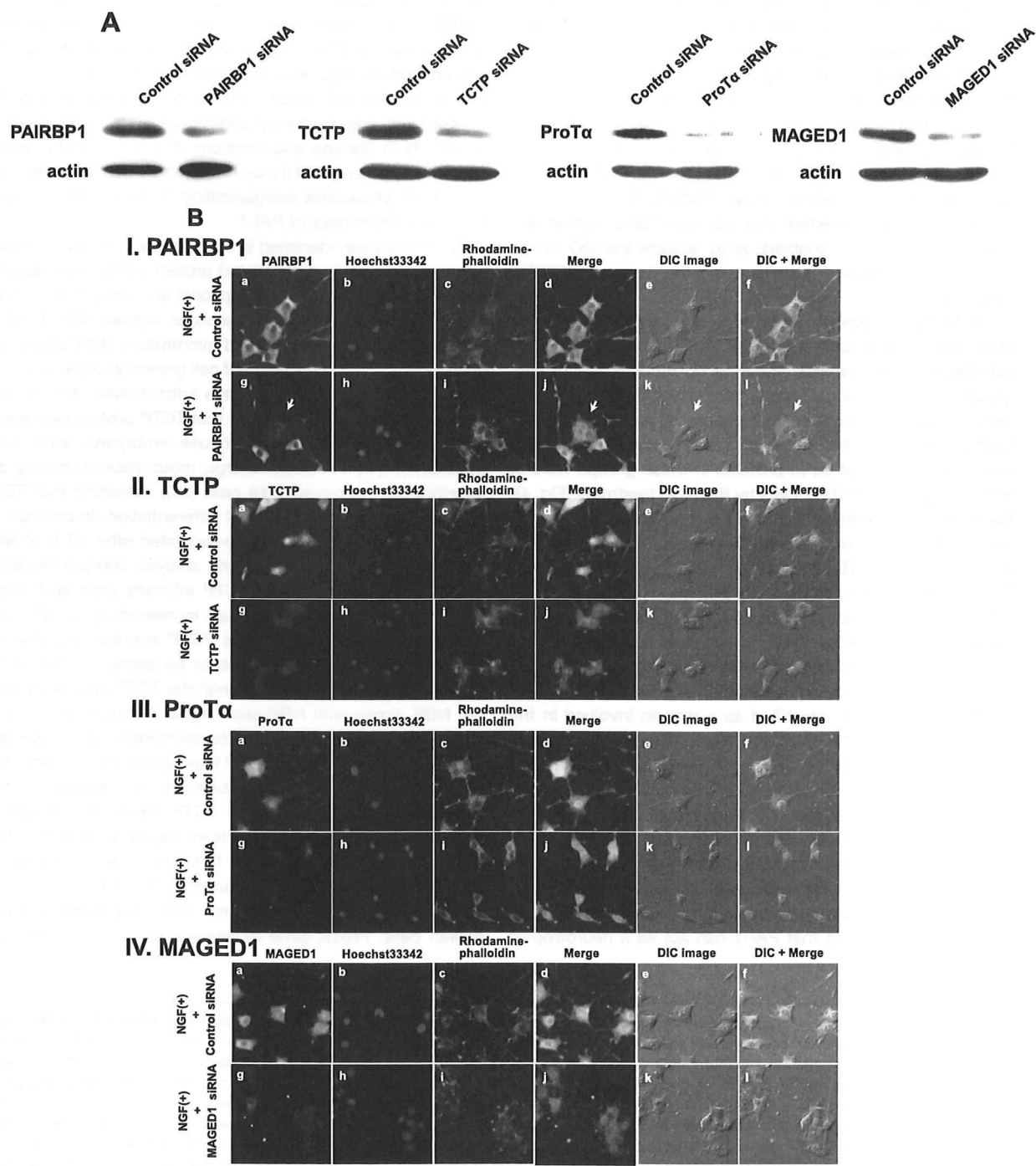


FIG. 6. The effects caused by the suppression of the NGF-inducible proteins on PC12 cell differentiation. A, the cells were transfected with siRNA for each NGF-inducible protein or control siRNA for 24 h and then treated with NGF for 48 h. Immunoblot images were taken after treatment with each siRNA of the protein. Down-regulation of these proteins was confirmed. B, the cells were transfected with siRNA for each NGF-inducible protein or control siRNA for 24 h and then treated with NGF for 48 h. Cells were fixed and incubated with the antibodies against the indicated proteins (I, PAIRBP1; II, TCTP; III, ProTa; and IV, MAGED1) followed by detection with Alexa Fluor 488-labeled secondary antibodies and observation with a fluorescence microscope (a and g). Nuclear and F-actin were stained with Hoechst33342 (b and h) and rhodamine-phalloidin (c and i), respectively. The merged images for a, b, c and g, h, i, are shown in d and j, respectively. The merged images

Downloaded from www.mcponline.org at KUMAMOTO UNIV on October 26, 2009

sisting of thousands of proteins cannot be easily annotated by GO because of the general lack of either an automated method of proteomics GO annotation or GO analysis software that directly links to the proteomics database. Second, the genome information (including GO) of rat is much poorer than that of human or mouse. To overcome those difficulties, we therefore created a simple method, namely the MANGO method, that consists of the annotation tool (MANGO) and our PC12 cell proteome reference set (PC12RPS) with all non-human proteins converted into corresponding human orthologs. This method enabled us to analyze the GO of the differentially expressed proteins using the human PC12RPS very quickly.

The MANGO method helped us to narrow the focus of our study when the results suggested that NGF-induced PC12 cell differentiation involves functional up-regulation of protein groups related to six processes from which we selected cell morphogenesis and apoptosis/cell survival for deeper investigation. This led to biological validation by Western blotting, which confirmed that all of proteins in these groups were in fact up-regulated in PC12 cells by the NGF treatment (Fig. 4). Because their neuronal functions have not been reported in detail, of the proteins shown in Fig. 4, we focused on PAIRBP1 (34, 35), TCTP (36), ProT α (37), and MAGED1 (38). The indispensable roles of these proteins were further indicated by our subsequent ICC and siRNA-based studies. In this way, our MANGO method allowed us to quickly determine high probability candidate proteins whose important roles in NGF-induced PC12 cell differentiation are elaborated below.

PAIRBP1 has been identified as a protein involved in the regulation of PAI-1 mRNA stability via its binding to the cyclic nucleotide-responsive sequence of the PAI-1 mRNA (34). PAI-1 is the primary inhibitor of both urokinase- and tissue-type plasminogen activator (47). Soeda *et al.* (35) have shown that PAI-1 promotes the neurite outgrowth and survival of PC12 cells. This neuroprotective activity is correlated with enhanced activation of both extracellular signal-regulated kinase following a direct phosphorylation of NGF receptor Trk A and c-Jun, suggesting that PAI-1 can act as a neurotrophic

factor (35). Based on those findings, we hypothesized that PAIRBP1 would be a positive regulator of PC12 differentiation and survival via PAI-1 mRNA stability. In our study, we observed that its suppression caused the inhibition of neurite formation and cell death. Interestingly PAIRBP1 was expressed not only in the cytoplasm but also in the neurites, especially in the tips and junctions (Fig. 5A, *g* and *i*, *arrowheads*), suggesting that it may have some other essential roles such as in cytoskeletal reorganization for the neurite formation that are independent of PAI-1.

TCTP has been identified in many eukaryotes and is widely expressed. It is a growth-related protein whose expression is highly regulated at the transcriptional and translational levels and by a wide range of extracellular signals (48). TCTP is involved in calcium binding and microtubule stabilization and is implicated in the regulation of cell growth and the cell cycle (48). It is also postulated to have antiapoptotic activity (49). Previous reports have revealed that TCTP protein expression decreased in differentiating mouse embryonic stem cells (mESCs) (50) and in dopaminergic motor neurons having differentiated from mouse E14 cells (36), indicating that TCTP has an important role in mESC differentiation. In contrast, in our iTRAQ data, TCTP was up-regulated after 48 h of NGF stimulation. Our Western blotting analysis showed the time-dependent changes of the TCTP intensity after NGF treatment; namely the intensities had increased up to 12 h and then gradually decreased. This TCTP expression pattern in NGF-treated PC12 cells seems to be similar to that of the developing mESC. Compared with the TCTP intensities without NGF, those with NGF were higher throughout the same analysis (12–72 h) (Fig. 4 and supplemental Fig. 2). We also showed in this study that TCTP knockdown caused inhibition of neurite formation and apoptosis (Fig. 6C), suggesting that NGF-induced up-regulation of TCTP could be a trigger of neurite outgrowth and that its down-regulation after this triggering role might have another function in the neurite formation or cell survival of NGF-induced PC12 cells.

ProT α is a highly acidic protein widely expressed in mammalian cells. ProT α gene expression is correlated with cell

for *d*, *e* and *j*, *k* are shown in *f* and *l*, respectively. Differential interference contrast (DIC) images of PC12 cells in the same field were shown in *e* and *k*. The suppression of expression of each protein led to significant morphological changes, such as inhibition of neurite formation and induction of cellular aggregation in differentiating PC12 cells. *Arrowheads* indicate the PAIRBP1-suppressed cells. *C*, effects on neurite outgrowth and survival of PC12 cells of the siRNA treatment of the NGF-inducible proteins. *a*, representative time lapse images of NGF-stimulated PC12 cells treated with each siRNA for NGF-inducible proteins. The cells were transfected with siRNA for each NGF-inducible protein or control siRNA and stimulated with NGF for 72 h. A significant inhibition of neurite formation was observed due to each siRNA treatment. *Arrows* show the apoptotic phenotypes of PC12 cells. *b* and *c*, the cells were transfected with siRNA for each NGF-inducible protein or control siRNA and stimulated with NGF for 48 h under the condition of low serum (1% horse serum). The average of the number and total length of neurites of the PC12 cells are shown on the *y* axis (*b* and *c*). The data are expressed as means and S.D. of the three independent experiments ($n = 3$). For each experiment, more than 50 cells were counted. *d* and *e*, effects on PC12 cell survival of the siRNA treatment of the NGF-inducible proteins. The cells were transfected with siRNA for each NGF-inducible protein or control siRNA, stimulated with NGF for 48 h, fixed, and stained with PI and Hoechst33342 dye. Representative images of PI and Hoechst staining of PC12 cells treated with each siRNA and control and stimulated with NGF are shown (*d*). The percentage of PI-positive PC12 cells in total Hoechst-stained PC12 cells is shown on the *y* axis (*e*). The data and *error bars* are expressed as means and S.D. of the three independent experiments ($n = 3$), respectively. For each experiment, more than 500 cells were counted. *, $p < 0.05$; **, $p < 0.01$; and ***, $p < 0.001$ versus NGF + control siRNA treatment (Student's *t* test).

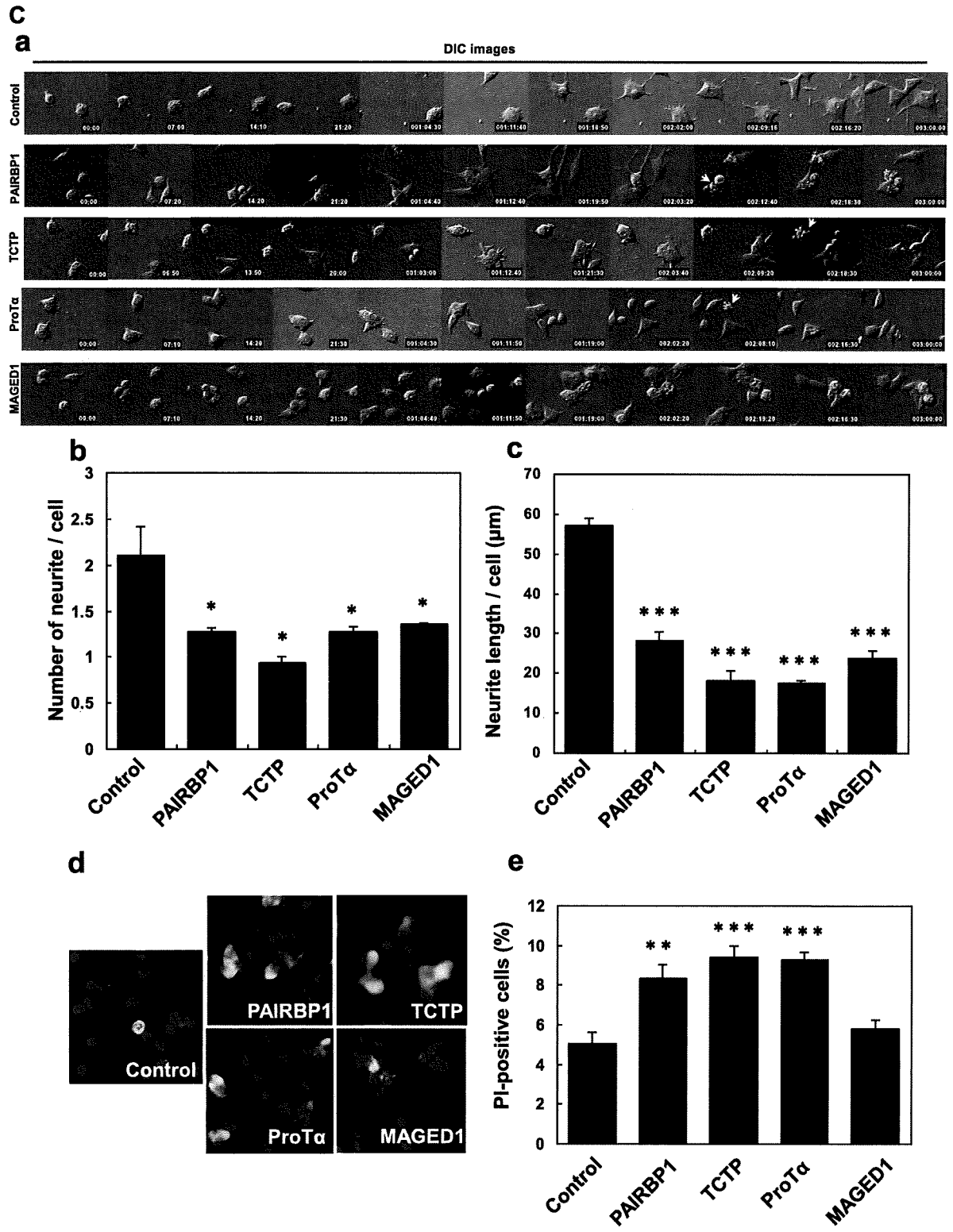


Fig. 6—continued

proliferation in a wide variety of cells, providing evidence for its involvement in cell growth (51). ProT α overexpression has been shown to both accelerate proliferation and retard differentiation in several cell types, such as HL60, K562, U937, and PC12 (37). Because ProT α was up-regulated in our proteomics analysis, we evaluated the time-dependent change in ProT α protein levels after NGF treatment by Western blotting (Fig. 4 and supplemental Fig. 2). ProT α expression peaked at 24 h and was followed by immediate down-regulation, suggesting that there might be some strict feedback mechanisms for ProT α expression in NGF-induced PC12 differentiation. Also ProT α was primarily localized in the nucleus after NGF stimulation (Fig. 5C, g and i, arrows). Nuclear ProT α reportedly interacts with histone H1 to promote chromatin decondensation and facilitate transcription or replication, the mechanism of which is regulated by casein kinase II phosphorylation of ProT α (52). Interestingly we observed that the expression of the casein kinase II catalytic subunit was down-regulated by NGF (Table I). The up-regulation of ProT α with accompanying casein kinase II down-regulation could therefore lead to transcriptional activation of genes related to PC12 cell differentiation and survival.

MAGED1, neurotrophin receptor-interacting MAGE homolog, was identified as a binding partner for p75 neurotrophin receptor (p75NTR) by yeast two-hybrid assay (38). MAGED1 reportedly binds p75NTR, antagonizes p75NTR to TrkA association, inhibits cell cycle progression, and facilitates p75NTR-mediated apoptosis (38). However, there is little information about p75NTR-mediated signaling by MAGED1. Because the localization of MAGED1 is not consistent with that of p75NTR (53), MAGED1 is likely to have the potential for signaling that is independent of p75NTR. Human MAGED1 reportedly regulates homotypic cell-cell adhesion by disrupting the E-cadherin- β -catenin complex (54). We observed the aggregation of differentiating PC12 cells triggered by the siRNA-induced MAGED1 down-regulation (Fig. 6, B, IV and C, a, and supplemental Movie 5), suggesting that MAGED1 suppression may have a significant effect on cell morphogenesis rather than cell survival during NGF-induced differentiation in PC12 cells.

In this study, we constructed the proteome database for PC12 cells containing the maximum number of the peptides/proteins so far identified and successfully identified new proteins related to cellular differentiation and apoptosis/survival. Our sequential proteomics strategy demonstrated here is simple and effective for identifying the proteins most likely involved in the physiological phenomena of interest because it enables one to quickly but confidently identify an appropriate focus on biological processes when interpreting extensive proteomics data. We expect that this proteomics strategy can become a standard method to target and elucidate the functions of proteins involved in cellular biological processes, to study the onset and pathogenesis of various diseases, and to discover new drug candidates in the near future.

Acknowledgments—We thank Prof. Hideyuki Saya, Keio University, School of Medicine, for kind advice and encouragement throughout this study. We also thank the entire staff of the Department of Tumor Genetics and Biology in Kumamoto University for helpful support, especially N. Tsubota, U. Midorikawa, and M. Nagayama for collaborative endeavors and M. Morikawa, M. Shimono, and C. Midorikawa for secretarial assistance. We are also grateful to staff members of the Proteomic Analysis Core-system on General Research Core Laboratory, Kumamoto University Medical School, for important contributions to the experiments.

* This work was supported by grants from Cancer Research (to N. A.), Kiban Research (to N. A.), and Houga Research (to N. A.) from the Ministry of Education, Culture, Sports, Science and Technology of Japan; from The Ministry of Health and Welfare of Japan (to N. A.); from the Japan Health Sciences Foundation (to D. K. and N. A.); and from the Center of Excellence project B of Kumamoto University for proteomics research and education (to N. A.).

□ The on-line version of this article (available at <http://www.mcponline.org>) contains supplemental material.

|| To whom correspondence should be addressed. Tel.: 81-96-373-5119; Fax: 81-96-373-5210; E-mail: nori@gpo.kumamoto-u.ac.jp.

REFERENCES

- Ross, P. L., Huang, Y. N., Marchese, J. N., Williamson, B., Parker, K., Hattan, S., Khainovski, N., Pillai, S., Dey, S., Daniels, S., Purkayastha, S., Juhasz, P., Martin, S., Bartlett-Jones, M., He, F., Jacobson, A., and Pappin, D. J. (2004) Multiplexed protein quantitation in *Saccharomyces cerevisiae* using amine-reactive isobaric tagging reagents. *Mol. Cell. Proteomics* **3**, 1154–1169
- Mann, M. (2006) Functional and quantitative proteomics using SILAC. *Nat. Rev. Mol. Cell Biol.* **7**, 952–958
- Keller, M., Rügge, A., Werner, S., and Beer, H. D. (2008) Active caspase-1 is a regulator of unconventional protein secretion. *Cell* **132**, 818–831
- Wang, Z., Gucek, M., and Hart, G. W. (2008) Cross-talk between GlcNAcylation and phosphorylation: site-specific phosphorylation dynamics in response to globally elevated O-GlcNAc. *Proc. Natl. Acad. Sci. U.S.A.* **105**, 13793–13798
- Graumann, J., Hubner, N. C., Kim, J. B., Ko, K., Moser, M., Kumar, C., Cox, J., Schöler, H., and Mann, M. (2008) Stable isotope labeling by amino acids in cell culture (SILAC) and proteome quantitation of mouse embryonic stem cells to a depth of 5,111 proteins. *Mol. Cell. Proteomics* **7**, 672–683
- DeSouza, L. V., Grigull, J., Ghanny, S., Dubé, V., Romaschin, A. D., Colgan, T. J., and Siu, K. W. (2007) Endometrial carcinoma biomarker discovery and verification using differentially tagged clinical samples with multidimensional liquid chromatography and tandem mass spectrometry. *Mol. Cell. Proteomics* **6**, 1170–1182
- Raihan, R., Desouza, L. V., Matta, A., Chandra Tripathi, S., Ghanny, S., Datta Gupta, S., Bahadur, S., and Siu, K. W. (2008) Discovery and verification of head-and-neck cancer biomarkers by differential protein expression analysis using iTRAQ labeling, multidimensional liquid chromatography, and tandem mass spectrometry. *Mol. Cell. Proteomics* **7**, 1162–1173
- Bantscheff, M., Eberhard, D., Abraham, Y., Bastuck, S., Boesche, M., Hobson, S., Mathieson, T., Perrin, J., Ralda, M., Rau, C., Reader, V., Sweetman, G., Bauer, A., Bouwmeester, T., Hopf, C., Kruse, U., Neubauer, G., Ramsden, N., Rick, J., Kuster, B., and Drewes, G. (2007) Quantitative chemical proteomics reveals mechanisms of action of clinical ABL kinase inhibitors. *Nat. Biotechnol.* **25**, 1035–1044
- Greene, L. A., and Tischler, A. S. (1976) Establishment of a noradrenergic clonal line of rat adrenal pheochromocytoma cells which respond to nerve growth factor. *Proc. Natl. Acad. Sci. U.S.A.* **73**, 2424–2428
- Adler, E. M. (2006) Teaching resources. Cell culture as a model system for teaching: using PC12 cells. *Sci. STKE* **2006**, tr5
- Yankner, B. A., Dawes, L. R., Fisher, S., Villa-Komaroff, L., Oster-Granite, M. L., and Neve, R. L. (1989) Neurotoxicity of a fragment of the amyloid precursor associated with Alzheimer's disease. *Science* **245**, 417–420
- Apostol, B. L., Kazantsev, A., Raffioni, S., Illes, K., Pallos, J., Bodai, L., Slepko, N., Bear, J. E., Gertler, F. B., Hersch, S., Housman, D. E., Marsh,

- J. L., and Thompson, L. M. (2003) A cell-based assay for aggregation inhibitors as therapeutics of polyglutamine-repeat disease and validation in *Drosophila*. *Proc. Natl. Acad. Sci. U.S.A.* **100**, 5950–5955
13. Ryu, E. J., Harding, H. P., Angelastro, J. M., Vitolo, O. V., Ron, D., and Greene, L. A. (2002) Endoplasmic reticulum stress and the unfolded protein response in cellular models of Parkinson's disease. *J. Neurosci.* **22**, 10690–10698
 14. Yunoue, S., Tokuo, H., Fukunaga, K., Feng, L., Ozawa, T., Nishi, T., Kikuchi, A., Hattori, S., Kuratsu, J., Saya, H., and Araki, N. (2003) Neurofibromatosis type I tumor suppressor neurofibromin regulates neuronal differentiation via its GTPase-activating protein function toward Ras. *J. Biol. Chem.* **278**, 26958–26969
 15. Feng, L., Yunoue, S., Tokuo, H., Ozawa, T., Zhang, D., Patrakitkomjorn, S., Ichimura, T., Saya, H., and Araki, N. (2004) PKA phosphorylation and 14-3-3 interaction regulate the function of neurofibromatosis type I tumor suppressor, neurofibromin. *FEBS Lett.* **557**, 275–282
 16. Patrakitkomjorn, S., Kobayashi, D., Morikawa, T., Wilson, M. M., Tsubota, N., Irie, A., Ozawa, T., Aoki, M., Arimura, N., Kaibuchi, K., Saya, H., and Araki, N. (2008) Neurofibromatosis type 1 (NF1) tumor suppressor, neurofibromin, regulates the neuronal differentiation of PC12 cells via its associating protein, CRMP-2. *J. Biol. Chem.* **283**, 9399–9413
 17. Davies, A. M. (1994) The role of neurotrophins in the developing nervous system. *J. Neurobiol.* **25**, 1334–1348
 18. Chao, M. V. (2003) Neurotrophins and their receptors: a convergence point for many signalling pathways. *Nat. Rev. Neurosci.* **4**, 299–309
 19. Lee, N. H., Weinstock, K. G., Kirkness, E. F., Earle-Hughes, J. A., Fuldner, R. A., Marmaros, S., Glodek, A., Gocayne, J. D., Adams, M. D., Kerlavage, A. R., Fraser, C. M., and Venter, J. C. (1995) Comparative expressed-sequence-tag analysis of differential gene expression profiles in PC-12 cells before and after nerve growth factor treatment. *Proc. Natl. Acad. Sci. U.S.A.* **92**, 8303–8307
 20. Mayumi, K., Yaoi, T., Kawai, J., Kojima, S., Watanabe, S., and Suzuki, H. (1998) Improved restriction landmark cDNA scanning and its application to global analysis of genes regulated by nerve growth factor in PC12 cells. *Biochim. Biophys. Acta* **1399**, 10–18
 21. Brown, A. J., Hutchings, C., Burke, J. F., and Mayne, L. V. (1999) Application of a rapid method (targeted display) for the identification of differentially expressed mRNAs following NGF-induced neuronal differentiation in PC12 cells. *Mol. Cell. Neurosci.* **13**, 119–130
 22. Angelastro, J. M., Klimaschewski, L., Tang, S., Vitolo, O. V., Weissman, T. A., Donlin, L. T., Shelanski, M. L., and Greene, L. A. (2000) Identification of diverse nerve growth factor-regulated genes by serial analysis of gene expression (SAGE) profiling. *Proc. Natl. Acad. Sci. U.S.A.* **97**, 10424–10429
 23. Dijkmans, T. F., van Hooijdonk, L. W., Schouten, T. G., Kamphorst, J. T., Vellinga, A. C., Meerman, J. H., Fitzsimons, C. P., de Kloet, E. R., and Vreugdenhil, E. (2008) Temporal and functional dynamics of the transcriptome during nerve growth factor-induced differentiation. *J. Neurochem.* **105**, 2388–2403
 24. Garrels, J. I., and Schubert, D. (1979) Modulation of protein synthesis by nerve growth factor. *J. Biol. Chem.* **254**, 7978–7985
 25. Sussman, M. A., Battenberg, E., Bloom, F. E., and Fowler, V. M. (1990) Identification of two nerve growth factor-induced polypeptides in PC12 cells. *J. Mol. Neurosci.* **2**, 163–174
 26. Huang, C. M., Shui, H. A., Wu, Y. T., Chu, P. W., Lin, K. G., Kao, L. S., and Chen, S. T. (2001) Proteomic analysis of proteins in PC12 cells before and after treatment with nerve growth factor: increased levels of a 43-kDa chromogranin B-derived fragment during neuronal differentiation. *Brain Res. Mol. Brain Res.* **92**, 181–192
 27. Huang, Y. H., Chang, A. Y., Huang, C. M., Huang, S. W., and Chan, S. H. (2002) Proteomic analysis of lipopolysaccharide-induced apoptosis in PC12 cells. *Proteomics* **2**, 1220–1228
 28. Zhou, B., Yang, W., Ji, J. G., and Ru, B. G. (2004) Differential display proteome analysis of PC-12 cells transiently transfected with metallothionein-3 gene. *J. Proteome Res.* **3**, 126–131
 29. Yang, W., Liu, P., Liu, Y., Wang, Q., Tong, Y., and Ji, J. (2006) Proteomic analysis of rat pheochromocytoma PC12 cells. *Proteomics* **6**, 2982–2990
 30. Shilov, I. V., Seymour, S. L., Patel, A. A., Loboda, A., Tang, W. H., Keating, S. P., Hunter, C. L., Nuwaysir, L. M., and Schaeffer, D. A. (2007) The Paragon Algorithm, a next generation search engine that uses sequence temperature values and feature probabilities to identify peptides from tandem mass spectra. *Mol. Cell. Proteomics* **6**, 1638–1655
 31. Carbon, S., Ireland, A., Mungall, C. J., Shu, S., Marshall, B., and Lewis, S. (2009) AmiGO: online access to ontology and annotation data. *Bioinformatics* **25**, 288–289
 32. Kondili, K., Tsolas, O., and Papamarcaki, T. (1996) Selective interaction between parathyrosin and histone H1. *Eur. J. Biochem.* **242**, 67–74
 33. Ueda, H., Fujita, R., Yoshida, A., Matsunaga, H., and Ueda, M. (2007) Identification of prothymosin-alpha1, the necrosis-apoptosis switch molecule in cortical neuronal cultures. *J. Cell Biol.* **176**, 853–862
 34. Heaton, J. H., Dlakic, W. M., Dlakic, M., and Gelehrter, T. D. (2001) Identification and cDNA cloning of a novel RNA-binding protein that interacts with the cyclic nucleotide-responsive sequence in the Type-1 plasminogen activator inhibitor mRNA. *J. Biol. Chem.* **276**, 3341–3347
 35. Soeda, S., Shinomiya, K., Ochiai, T., Koyanagi, S., Toda, A., Eyanagi, R., and Shimeno, H. (2006) Plasminogen activator inhibitor-1 aids nerve growth factor-induced differentiation and survival of pheochromocytoma cells by activating both the extracellular signal-regulated kinase and c-Jun pathways. *Neuroscience* **141**, 101–108
 36. Wang, D., and Gao, L. (2005) Proteomic analysis of neural differentiation of mouse embryonic stem cells. *Proteomics* **5**, 4414–4426
 37. Rodríguez, P., Viñuela, J. E., Alvarez-Fernández, L., Buceta, M., Vidal, A., Domínguez, F., and Gómez-Márquez, J. (1998) Overexpression of prothymosin alpha accelerates proliferation and retards differentiation in HL-60 cells. *Biochem. J.* **331**, 753–761
 38. Salehi, A. H., Roux, P. P., Kubu, C. J., Zeindler, C., Bhakar, A., Tannis, L. L., Verdi, J. M., and Barker, P. A. (2000) NRAGE, a novel MAGE protein, interacts with the p75 neurotrophin receptor and facilitates nerve growth factor-dependent apoptosis. *Neuron* **27**, 279–288
 39. Stapels, M. D., and Barofsky, D. F. (2004) Complementary use of MALDI and ESI for the HPLC-MS/MS analysis of DNA-binding proteins. *Anal. Chem.* **76**, 5423–5430
 40. Possenti, R., Eldridge, J. D., Paterson, B. M., Grasso, A., and Levi, A. (1989) A protein induced by NGF in PC12 cells is stored in secretory vesicles and released through the regulated pathway. *EMBO J.* **8**, 2217–2223
 41. Mobarak, C. D., Anderson, K. D., Morin, M., Beckel-Mitchener, A., Rogers, S. L., Furneaux, H., King, P., and Perone-Bizzozero, N. I. (2000) The RNA-binding protein HuD is required for GAP-43 mRNA stability, GAP-43 gene expression, and PKC-dependent neurite outgrowth in PC12 cells. *Mol. Biol. Cell* **11**, 3191–3203
 42. Laslop, A., and Tschernitz, C. (1992) Effects of nerve growth factor on the biosynthesis of chromogranin A and B, secretogranin II and carboxypeptidase H in rat PC12 cells. *Neuroscience* **49**, 443–450
 43. Jacovina, A. T., Zhong, F., Khazanova, E., Lev, E., Deora, A. B., and Hajjar, K. A. (2001) Neuritogenesis and the nerve growth factor-induced differentiation of PC-12 cells requires annexin II-mediated plasmin generation. *J. Biol. Chem.* **276**, 49350–49358
 44. Aletta, J. M., Angeletti, R., Liem, R. K., Purcell, C., Shelanski, M. L., and Greene, L. A. (1988) Relationship between the nerve growth factor-regulated clone 73 gene product and the 58-kilodalton neuronal intermediate filament protein (peripherin). *J. Neurochem.* **51**, 1317–1320
 45. Stroth, U., Meffert, S., Gallinat, S., and Unger, T. (1998) Angiotensin II and NGF differentially influence microtubule proteins in PC12W cells: role of the AT2 receptor. *Brain Res. Mol. Brain Res.* **53**, 187–195
 46. Lorusso, A., Covino, C., Priori, G., Bachi, A., Meldolesi, J., and Chiarelli, E. (2006) Annexin2 coating the surface of enlargosomes is needed for their regulated exocytosis. *EMBO J.* **25**, 5443–5456
 47. Lawrence, D. A., Strandberg, L., Ericson, J., and Ny, T. (1990) Structure-function studies of the SERPIN plasminogen activator inhibitor type 1. Analysis of chimeric strained loop mutants. *J. Biol. Chem.* **265**, 20293–20301
 48. Bommer, U. A., and Thiele, B. J. (2004) The translationally controlled tumour protein (TCTP). *Int. J. Biochem. Cell Biol.* **36**, 379–385
 49. Yang, Y., Yang, F., Xiong, Z., Yan, Y., Wang, X., Nishino, M., Mirkovic, D., Nguyen, J., Wang, H., and Yang, X. F. (2005) An N-terminal region of translationally controlled tumor protein is required for its antiapoptotic activity. *Oncogene* **24**, 4778–4788
 50. Baharvand, H., Fathi, A., Gourabi, H., Mollamohammadi, S., and Salekdeh, G. H. (2008) Identification of mouse embryonic stem cell-associated proteins. *J. Proteome Res.* **7**, 412–423
 51. Segade, F., and Gómez-Márquez, J. (1999) Prothymosin alpha. *Int. J. Biochem. Cell Biol.* **31**, 1243–1248



52. Gómez-Márquez, J. (2007) Function of prothymosin alpha in chromatin decondensation and expression of thymosin beta-4 linked to angiogenesis and synaptic plasticity. *Ann. N.Y. Acad. Sci.* **1112**, 201–209
53. Barrett, G. L., Greferath, U., Barker, P. A., Trieu, J., and Bennie, A. (2005) Co-expression of the P75 neurotrophin receptor and neurotrophin receptor-interacting melanoma antigen homolog in the mature rat brain. *Neuroscience* **133**, 381–392
54. Xue, B., Wen, C., Shi, Y., Zhao, D., and Li, C. (2005) Human NRAGE disrupts E-cadherin/beta-catenin regulated homotypic cell-cell adhesion. *Biochem. Biophys. Res. Commun.* **336**, 247–251
55. Quinn, C. C., Chen, E., Kinjo, T. G., Kelly, G., Bell, A. W., Elliott, R. C., McPherson, P. S., and Hockfield, S. (2003) TUC-4b, a novel TUC family variant, regulates neurite outgrowth and associates with vesicles in the growth cone. *J. Neurosci.* **23**, 2815–2823

Contribution of BCR-ABL-independent activation of ERK1/2 to acquired imatinib resistance in K562 chronic myeloid leukemia cells

Takeru Nambu,¹ Norie Araki,^{2,5} Aiko Nakagawa,¹ Akihiko Kuniyasu,³ Tatsuya Kawaguchi,⁴ Akinobu Hamada¹ and Hideyuki Saito^{1,5}

¹Department of Pharmacy, Kumamoto University Hospital, Kumamoto; ²Department of Tumor Genetics and Biology, Graduate School of Medical Sciences, Kumamoto University School of Medicine, Kumamoto; ³Department of Molecular Cell Function, Graduate School of Pharmaceutical Sciences, Kumamoto University, Kumamoto; ⁴Department of Hematology and Infectious Diseases, Kumamoto University Hospital, Kumamoto, Japan

(Received July 3, 2009/Revised September 4, 2009/Accepted September 8, 2009/Online publication October 14, 2009)

BCR-ABL tyrosine kinase, generated from the reciprocal chromosomal translocation t(9;22), causes chronic myeloid leukemia (CML). BCR-ABL is inhibited by imatinib; however, several mechanisms of imatinib resistance have been proposed that account for loss of imatinib efficacy in patients with CML. Previously, we showed that overexpression of the efflux drug transporter P-glycoprotein partially contributed to imatinib resistance in imatinib-resistant K562 CML cells having no BCR-ABL mutations. To explain an additional mechanism of drug resistance, we established a subclone (K562/R) of the cells and examined the BCR-ABL signaling pathway in these and wild-type K562 (K562/W) cells. We found the K562/R cells were 15 times more resistant to imatinib than their wild-type counterparts. In both cell lines, BCR-ABL and its downstream signaling molecules, such as ERK1/2, ERK5, STAT5, and AKT, were phosphorylated in the absence of imatinib. In both cell lines, imatinib effectively reduced the phosphorylation of all the above, except ERK1/2, whose phosphorylation was, interestingly, only inhibited in the wild-type cells. We then observed that phospho-ERK1/2 levels decreased in the presence of siRNA targeting BCR-ABL, again, only in the K562/W cells. However, using an ERK1/2 inhibitor, U0126, we found that we could reduce phospho-ERK1/2 levels in K562/R cells and restore their sensitivity to imatinib. Taken together, we conclude that the BCR-ABL-independent activation of ERK1/2 contributes to imatinib resistance in K562/R cells, and that ERK1/2 could be a target for the treatment of CML patients whose imatinib resistance is due to this mechanism. (*Cancer Sci* 2010; 101: 137-142)

Chronic myeloid leukemia, a hematopoietic stem cell disorder, is characterized by the expression of the chimeric BCR-ABL oncoprotein, caused by the reciprocal chromosomal translocation t(9;22) (q34;q11), which generates a shortened chromosome 22 or Philadelphia chromosome.⁽¹⁾ BCR-ABL is a cytoplasmic protein with constitutive tyrosine kinase activity responsible for transformation and leukemogenic effects. BCR-ABL is the target of the tyrosine kinase inhibitor imatinib, which also inhibits c-kit protooncogene/CD117 (c-KIT) and platelet-derived growth factor receptor (PDGFR).⁽²⁾ More than 90% of chronic-phase CML patients respond to imatinib, at least initially, and a high percentage of them achieve cytogenetic complete responses.⁽³⁾ However, some patients fail to respond to treatment with imatinib in front-line therapy (primary resistance), while others stop responding after an initial response (acquired resistance).⁽⁴⁾ Frequent clinical relevancies to imatinib resistance include point mutations in the *ABL* gene^(5,6) and amplification of the *BCR-ABL* fusion gene.⁽⁷⁾ In addition to these BCR-ABL-dependent mechanisms, BCR-ABL-independent mechanisms of imatinib resistance have been proposed,

which involve the drug transporter P-gp (MDR1, ATP-binding cassette subfamily B1 (ABCB1)),⁽⁸⁻¹⁰⁾ the drug carrier serum α_1 acid glycoprotein,⁽¹¹⁾ and signal cascades via LYN kinase.^(12,13) Although some mechanisms of imatinib resistance are understood, resistance to this drug is still an important challenge confronting the effective treatment of CML.

We previously focused on drug transporters and reported the potential contribution to imatinib resistance of P-gp, a multidrug efflux transporter, using K562 cells, which are known as a representative human CML cell line.⁽⁹⁾ In a previous study, we established imatinib-resistant K562 (prevK562/R) cells, which had wild-type BCR-ABL and overexpressed P-gp. In prevK562/R cells, intracellular imatinib levels were 42% less than those in wild-type K562 (K562/W) cells. Intracellular imatinib accumulation was restored completely by CysA, a P-gp inhibitor; however, CysA did not completely overcome prevK562/R cell sensitivity to imatinib. Therefore, we assumed that another mechanism was also involved in imatinib resistance in K562 cells. To identify this unknown mechanism, we focused on signal transduction pathways that were downstream of BCR-ABL, and analyzed imatinib resistance factors, other than overexpression of P-gp, using a new imatinib-resistant subclone of K562 (K562/R) cells, which was cloned from prevK562/R cells.

BCR-ABL has multiple downstream survival pathways, including ERK1/2, ERK5, AKT, JAK/STAT, nuclear factor kappa beta (NF- κ B), and BCL-xL.⁽¹⁴⁻¹⁸⁾ Phosphorylation of tyrosine 177 of BCR-ABL is necessary for binding of the adaptor growth factor receptor-bound protein (GRB2) to BCR-ABL, which involves the recruitment of son of sevenless (SOS), the nucleotide exchange factor of RAS.⁽¹⁹⁾ RAS activates both the RAF-MEK-ERK1/2 and PI3K-AKT pathways, which are engaged in cell survival and anti-apoptosis.^(18,20) ERK5, like ERK1/2, is a member of the mitogen-activated protein kinase family, is modulated by BCR-ABL, and contributes to the survival of leukemia cells.^(17,21) In the present study, we investigated the contributions of these downstream factors to imatinib resistance in K562/R cells.

Here, we demonstrate that BCR-ABL-independent activation of ERK1/2 may contribute to imatinib resistance in certain CML cell lines. This resistance can be overcome by co-treatment with the specific ERK1/2 inhibitor and imatinib, indicating that this co-treatment may be effective for imatinib-resistant CML patients.

Materials and Methods

Cell culture and cloning of imatinib-resistant K562 cells. K562/W cells were cultured in RPMI-1640 medium supplemented with

⁵To whom correspondence should be addressed.
E-mail: saitohide@fc.kuh.kumamoto-u.ac.jp; nori@gpo.kumamoto-u.ac.jp

10% FBS under an atmosphere of 5% CO₂-95% air at 37°C. prevK562/R cells were established by exposing gradually increasing concentrations of imatinib (from 0.3 to 10 μM) from K562/W cells.⁽⁹⁾ The new clonal cell line K562/R was established by limiting dilution from prevK562/R cells. K562/R cells were maintained under the same culture conditions in the presence of 1 μM imatinib.

mRNA isolation and cDNA synthesis. For mRNA extraction, MagNA Pure LC mRNA Isolation Kit II (Roche Diagnostics, Basel, Switzerland) was used as per the instruction manual. cDNA was synthesized by reverse transcription using the High-Capacity cDNA Archive Kit (Applied Biosystems, Foster City, CA, USA). Each prepared cellular cDNA was stored at -30°C.

Mutation analysis of the BCR-ABL kinase domain and KRAS. The kinase domain of BCR-ABL was amplified by PCR using each cellular cDNA.⁽⁹⁾ For the primary PCR, we used the forward primer 5'-CCAGCTGTCCACAGCATTC-3' and the reverse primer 5'-ATGGTCCAGAGGATCGCTCTCT-3', and for the secondary PCR, the forward primer 5'-GGGAGGGTGTACCATTACAGG-3' and the reverse primer, 5'-GCTGTGTAGG-TGTCCCCTGT-3', or the forward primer 5'-CCACTTGGTGAAGGTAGCTG-3' and the reverse primer, 5'-CCTGCAGCAAGGTAGTCA-3', were used. The analysis was carried out by DNA sequencing using an Applied Biosystems 3130 Genetic Analyzer. For the mutation analysis of KRAS ORF, the forward primer 5'-CGGGAGAGAGCCCTGCTG-3' and the reverse primer 5'-CCACTTGTACTAGTATGCCT-3' were used in PCR amplification. The sequence of the KRAS gene was analyzed by the Sigma-Aldrich DNA sequencing Service.

Cytotoxicity assay. The individual or combined cytotoxicities of imatinib and U0126 were determined by the Alamar Blue assay as described previously.^(9,22) Absorbance in cells without drug treatment was 100%.

Western blot analysis. K562/W and K562/R cells were homogenized in a solution containing 7 M urea, 2 M thiourea, 4% CHAPS, protease inhibitor cocktail (P8430; Sigma-Aldrich, St Louis, MO, USA), 2 mM Na₂VO₄, 10 mM NaF, 1 μM okadaic acid, and 1 mM DTT, using Micropestle (Eppendorf, Westbury, NY, USA). Crude membrane fraction selection and Western blotting conditions were as described previously.⁽⁹⁾ The following primary antibodies were used: LYN, phospho-STAT5 (Tyr⁶⁹⁴), STAT5 (BD Transduction Laboratories, Lexington, KY, USA), β-actin (Sigma-Aldrich), 4G10, Na⁺/K⁺ ATPase α-1 (Upstate Biotechnology, Lake Placid, NY, USA), c-ABL (Santa Cruz Biotechnology, Santa Cruz, CA, USA), phospho-ERK1/2, ERK1/2, phospho-AKT (Thr³⁰⁸), phospho-AKT (Ser⁴⁷³), AKT, ERK5 (Cell Signaling Technology, Beverly, MA, USA), and P-gp (C219 monoclonal antibody; Signet Laboratories, Dedham, MA, USA).

Two-dimensional Western blotting. Samples were desalted using the 2-D Clean-Up kit (GE Healthcare, Amersham Place, UK) and resolved with sample buffer (7 M urea, 2 M thiourea, 4% CHAPS, 0.5% IPG Buffer pH 3-10, and Destreaking buffer). The first-dimensional isoelectric focusing (pH 3-10, 7 cm) was carried out using the Ettan IPGPhor Cup Loading Manifold electrophoresis system (GE Healthcare) as per manufacturer recommendations. After reduction and alkylation of disulfide bonds with 10 mg/mL DTT and 25 mg/mL iodoacetamide, respectively, the second-dimensional separation was carried out by 12% SDS-PAGE. The 2D gel was immunoblotted as indicated above.

Real-time RT-PCR analysis. To determine the expression levels of *hMDR1* and *hβ-ACTIN* in the cells, we carried out TaqMan quantitative real-time RT-PCR using the ABI PRISM 7900 sequence detection system (Applied Biosystems), using the manufacturer's standard protocol (*hMDR1*, Hs00184491_m1; *hβ-ACTIN*, 4310881E).

Analysis of intracellular imatinib accumulation. Cells (2 × 10⁶) were incubated in 5 mL incubation buffer (150 mM NaCl, 3 mM

KCl, 1 mM CaCl₂, 0.5 mM MgCl₂, 5 mM D-glucose, 5 mM HEPES, pH 7.4) containing 1 μM imatinib. The cell pellet was washed once in ice-cold PBS containing 1% BSA, and twice with ice-cold PBS. The cellular imatinib was then extracted by incubation with 300 μL of 50% methanol (HPLC mobile phase/methanol = 1/1) for 30 min. Quantification of imatinib was done using the HPLC (model LC-6A; Shimadzu, Kyoto, Japan) method described previously.⁽⁸⁾ For the cellular protein quantitation, the pellet was solubilized with 200 μL of 1 N NaOH and analyzed by the Bradford method, using a Bio Rad Protein Assay kit (Bio Rad, Hercules, CA, USA) with BSA as a standard.

siRNA transfection. An siRNA specific for the b3a2 breakpoint of the BCR-ABL gene (5'-GCAGAGUUCAAAAGCCCUUdTdT), and a control siRNA composed of the scrambled b3a2 sequence (5'-GCAGAGUUCUAAAAGCGCUUdTdT),⁽²³⁾ were synthesized by Nippon EGT (Toyama, Japan). For electroporation of K562/W and K562/R cells, we used MicroPorator MP-100 (AR Brown, Tokyo, Japan). Cells were washed twice with PBS, and mixed with 20 μM stock siRNA to a final concentration of 3, 4 or 8 pmol/μL. Subsequently, 5 × 10⁵ cells/10 μL of the cell suspension were electroporated using the following settings: pulse voltage = 1450 V, pulse width = 10 ms, and pulse number = three times. After electroporation, the cells were resuspended in RPMI-1640 medium and cultured in the incubator for 48 h under the same conditions as other cells.

Statistical analysis. Statistical significance was determined by Welch's *t*-test. *P* < 0.05 was considered statistically significant.

Results

Characterization of imatinib-resistant K562/R cells. We established a new K562/R clonal cell line, which indicated a 15-fold increase in the IC₅₀ of imatinib over the parent K562/W cells (Fig. 1A), had no mutation in the BCR-ABL kinase domain (data not shown), and had neither overexpression nor overactivation of BCR-ABL or LYN kinase (Fig. 1B). Mutation analysis of KRAS showed no missense mutations^(24,25) in either cell line, although one silent mutation (519T > C) was found in both cells (Supporting information Fig. S1), suggesting that KRAS mutation in K562/R cells is not a factor in imatinib resistance. Both levels of mRNA (300-fold, *P* < 0.01; Fig. 1C) and protein in the crude membrane fraction (Supporting information Fig. S2B) of MDR1 were found to be elevated in K562/R cells compared with K562/W cells (almost similar results were obtained in prevK562/R cells⁽⁹⁾), although intracellular accumulation levels of imatinib were similar (Fig. 1D). Moreover, CysA, a P-gp inhibitor, did not influence intracellular imatinib accumulation levels in either type of cell. These results suggest that the imatinib resistance of K562/R cells is not directly related to the cellular P-gp expression level or function.

Imatinib did not inhibit the phosphorylation of ERK1/2 in K562/R cells. To study the specific activation signals in K562/R cells, K562/W and K562/R cells were treated with imatinib for varying lengths of time, as shown in Figure 2(A), after which the phosphorylation of BCR-ABL and its downstream factors, AKT, ERK5, STAT5, and ERK1/2 was examined. The phosphorylation levels of BCR-ABL and STAT5 were similarly high in both cell lines, but those of AKT and ERK1/2 were higher in the K562/R cells. After the treatment with imatinib, the phosphorylation of BCR-ABL, AKT, and STAT5 was effectively inhibited in both cell lines (Fig. 2A). ERK5 expression, which is known to be regulated by BCR-ABL,⁽¹⁷⁾ was not decreased by imatinib in either cell line (Fig. 2A). To analyze the phosphorylation status of ERK5 in both cell lines, we carried out 2D Western blotting using anti-ERK5 antibodies after a 24-h treatment

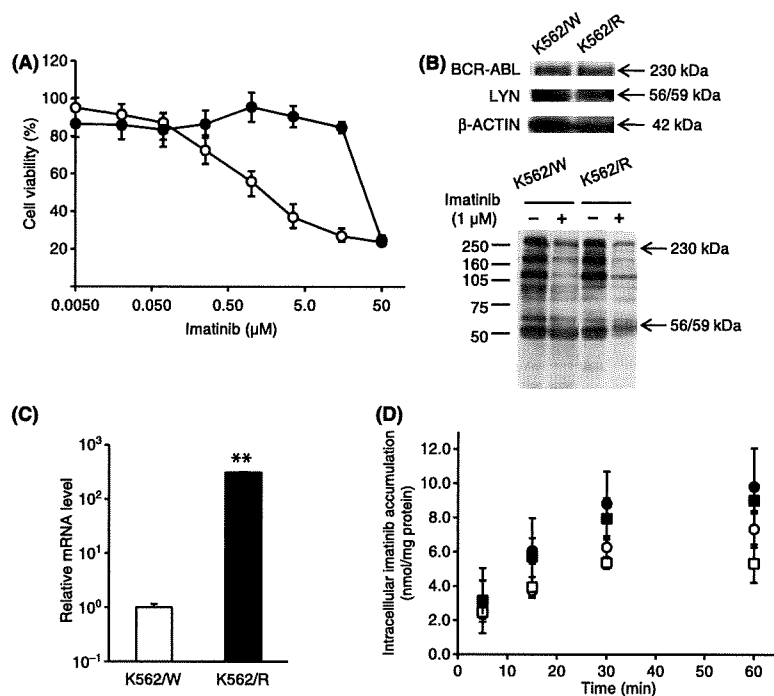


Fig. 1. Characteristics of imatinib-resistant K562/R cells. Imatinib and FBS were depleted from the medium 1 day before all experimental procedures to efflux intracellular imatinib from K562/R cells. (A) K562/W (open circles) and K562/R (closed circles) cells were exposed to various concentrations of imatinib for 48 h. Cell viability was assayed by Alamar Blue. Each point represents the mean \pm SD from six cells. (B) The expression levels of BCR-ABL, LYN, and β -actin and phosphorylation of tyrosine were examined by Western blot analysis. K562/W and K562/R cells were treated with 1 μ M imatinib for 15 min. (C) The mRNA levels of *hMDR1* and *h β -ACTIN* were examined by real time RT-PCR analysis. The relative amount of *hMDR1* mRNA was normalized to that of *h β -ACTIN*. (D) Intracellular imatinib accumulation was measured by HPLC analysis in K562/W and K562/R cells. The cells (2.0×10^5) were exposed to 1 μ M imatinib with (squares) or without (circles) 5 μ M cyclosporin A (CysA) at 37°C for varying lengths of time in K562/W (open symbols) and K562/R (closed symbols). Each point represents the mean \pm SD from four cells. ** $P < 0.01$ versus K562/W cells.

with imatinib, and compared the 2D patterns of ERK5-positive spots (Fig. 2C). Prior to imatinib treatment, both cell lines showed at least two ERK5-positive spots in 2D Western blotting. After treatment, one of these spots, presumed to be phosphorylated ERK5, underwent a significant shift from left (acid, pI 4.7) to right (basic, pI 4.9), suggesting that the phosphorylation of ERK5 was inhibited by the imatinib treatment in both cell lines. In contrast, ERK1/2 phosphorylation was inhibited in K562/W cells only (Fig. 2A). Interestingly, imatinib inhibitory effects on the phosphorylation of BCR-ABL were significant in a dose-dependent manner, while phosphorylation of ERK1/2 was never downregulated by imatinib in K562/R cells (Fig. 2B). Results similar to the above were obtained in prevK562/R cells (Supporting information Fig. S2A) and eight other clones also established as imatinib-resistant K562 cells (Fig. 2D). These results strongly indicate that, unlike in K562/W cells, BCR-ABL does not play a major role in the phosphorylation of ERK1/2 in K562/R cells.

BCR-ABL-targeting siRNA decreased the phosphorylation of ERK1/2 in K562/W cells, but not in K562/R cells. To confirm that ERK1/2 was activated independently of BCR-ABL in K562/R cells, BCR-ABL-targeting siRNA was transfected into cells from both cell lines. Since K562 cells express the b3a2 form of the BCR-ABL fusion mRNA, the specific sequence for b3a2 can effectively silence cellular BCR-ABL expression.⁽²³⁾ Transient transfection with varying amounts of b3a2 BCR-ABL siRNA significantly reduced the expression of BCR-ABL protein but not that of c-ABL in K562/W cells, compared with cells transfected with a control scrambled siRNA (Fig. 3A). The same treatment also induced the downregulation of phosphory-

lated-ERK1/2 in K562/W cells; however, it did not have this effect on K562/R cells (Fig. 3B).

Inhibition of ERK1/2 overcame imatinib resistance in K562/R cells. Because the results obtained from the above experiments strongly suggested that the BCR-ABL-independent activation of ERK1/2 is directly related to the mechanism of imatinib resistance in K562/R cells, we examined the effect of ERK1/2 inhibition on these cells. Treatment with an ERK1/2 inhibitor, U0126,⁽²⁶⁾ alone for 48 h showed similar dose-dependent toxicity for K562/W and K562/R cells (Fig. 4A). Treatment with U0126 (1 μ M) alone had little cytotoxic effect on either cells; however, in combination with imatinib, cell death increased dramatically, with both cells showing a similar sensitivity to imatinib (Fig. 4B). These results suggest that co-administration of the ERK1/2 inhibitor with imatinib could overcome imatinib resistance in K562/R cells.

Co-treatment of imatinib and U0126 inhibited phosphorylation of ERK1/2 in both K562/W and K562/R cells. Because co-administration of imatinib with U0126 restored imatinib sensitivity in K562/R cells, we next analyzed the inhibitory effect of imatinib on ERK1/2 phosphorylation by Western blotting in both cell lines exposed to U0126 alone or combined with imatinib. After U0126 treatment for 24 h, a dose-dependent downregulation of ERK1/2 phosphorylation in both cell lines was observed (Fig. 5). Interestingly, co-administration of 1 μ M imatinib with 1 μ M U0126 remarkably inhibited the phosphorylation of ERK1/2 in K562/R cells. These results confirm that the BCR-ABL-independent ERK1/2 activation is essential for imatinib resistance in K562/R cells.

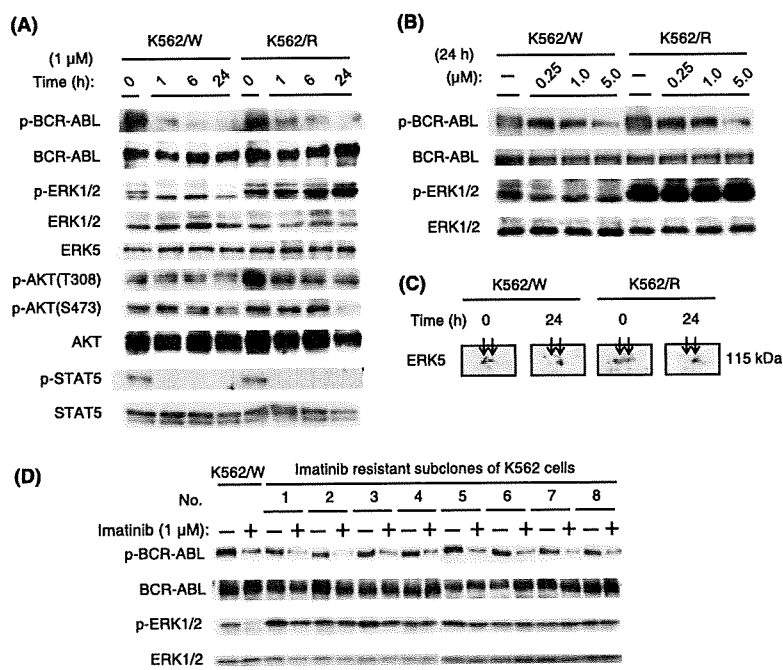


Fig. 2. Effects of imatinib on K562/W and K562/R cells were analyzed by immunoblotting. (A) Time course of BCR-ABL, ERK1/2, AKT, and STAT5 phosphorylation levels in K562/W and K562/R cells after 1 μM imatinib treatment. (B) Effect of the indicated concentrations of imatinib treatment for 24 h on the phosphorylation levels of BCR-ABL and ERK1/2 in K562/W and K562/R cells. (C) K562/W and K562/R cells were treated with 1 μM imatinib for 24 h. ERK5 was detected by 2D Western blotting. (D) K562/W and subcloned, imatinib-resistant K562 cells (from 1 to 8) were treated with 1 μM imatinib for 15 min. Clone cells of no. 2 is K562/R cells.

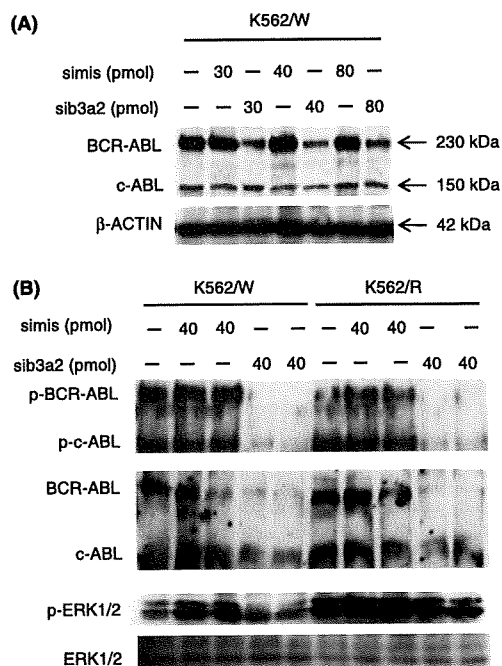


Fig. 3. Effects of BCR-ABL targeting siRNA on K562/W and K562/R cells. (A) K562/W cells were electroporated with different amounts of siRNA ranging from 30 to 80 pmol per 5×10^5 cells. (B) Effect of 40 pmol siRNA on the phosphorylation levels of BCR-ABL and ERK1/2 in K562/W and K562/R cells. sib3a2 and simis indicate BCR-ABL-specific siRNA and mismatch control siRNA, respectively.

Discussion

Despite the significant efficacy of imatinib in treating CML, the development of primary and acquired imatinib resistance is a problem in patients with CML. We previously reported that,

although P-gp partly contributes to imatinib resistance in prevK562/R cells, P-gp function alone cannot fully explain the resistance to imatinib. We thus postulated the involvement of a separate mechanism, and established a new imatinib-resistant K562 clonal cell line (K562/R) from prevK562/R cells for use in studying this mechanism. In the new clonal cells, BCR-ABL was inhibited by both imatinib and BCR-ABL siRNA, while neither treatment suppressed ERK1/2 phosphorylation. Co-treatment with imatinib and the ERK1/2 inhibitor U0126 restored imatinib sensitivity in K562/R cells. These data suggested for the first time that ERK1/2, activated through a BCR-ABL-independent pathway, contributes to imatinib resistance in K562 cells.

Imatinib resistance is most often caused by BCR-ABL-dependent mechanisms, including point mutations in the functional kinase domain of BCR-ABL^(5,6) and amplification of the BCR-ABL fusion gene.⁽⁷⁾ Point mutations in BCR-ABL reduce the binding of imatinib to the protein by either a direct or an indirect mechanism. However, in our study, the K562/R cells showed neither BCR-ABL mutations nor overexpression (Fig. 1B), indicating that their imatinib resistance mechanism could involve a BCR-ABL-independent pathway. Similar mechanisms have been reported, namely, the overexpression of P-gp and LYN kinase.⁽¹⁰⁻¹³⁾ Constitutively active mutants of KRAS are also known to be related to drug resistance in several cancers, including CML.^(24,25,27-29) For example, mutations in KRAS codon 12 involving a substitution of valine for glycine or aspartic acid are known; however, these were not observed in our K562/W or K562/R cells. Although both cell lines had the 519T > C silent mutation at the translated region (Supporting information Fig. S1), this particular mutation would not seem to influence the sensitivity to imatinib. In addition, LYN, which is a member of the Src tyrosine kinase family and is reported to be involved in imatinib resistance through overexpression of the anti-apoptotic protein BCL-2,^(12,13) is neither overexpressed nor overactivated in K562/R cells (Fig. 1B).

It is well known that imatinib interacts with P-gp as a substrate, and that overexpressed P-gp inhibits intracellular accumulation of imatinib.⁽⁸⁻¹⁰⁾ In our study, although MDR1 mRNA and protein expression were higher in K562/R than K562/W

Fig. 4. Cytotoxicity of U0126 alone and cotreatment with imatinib in K562/W and K562/R cells. (A) K562/W (open triangles) and K562/R (closed triangles) cells were exposed to 0.0050 μM U0126 alone for 48 h. (B) K562/W (open symbols) and K562/R (closed symbols) cells were exposed to 0.0050–50 μM imatinib with (squares) or without (circles) 1 μM U0126 for 48 h. Cell viability was assayed by Alamar Blue. Each point represents the mean \pm SD from six cells.

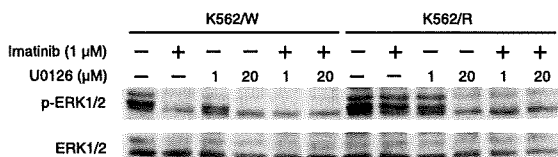
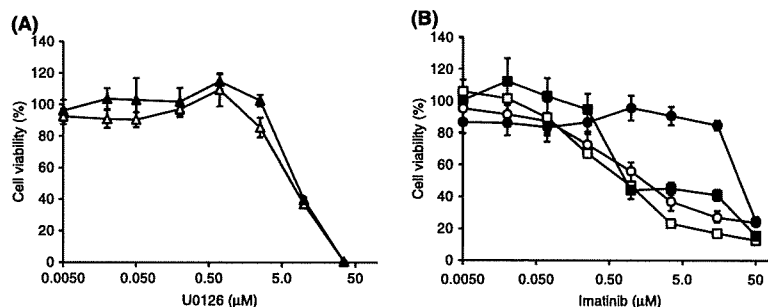


Fig. 5. The effects of imatinib and U0126, alone or in combination, on ERK1/2 phosphorylation. K562/W and K562/R cells were treated with or without 1 μM imatinib and U0126 (1 and 20 μM) for 24 h, as indicated.

cells, there was no difference in intracellular imatinib accumulation, which was not decreased by the P-gp inhibitor CysA (Fig. 1C,D). From these results, we hypothesized that P-gp functional activity was modulated by unknown factors in K562/R cells. Intracellular imatinib levels are possibly controlled by many factors, such as drug transporters and plasma carrier proteins, *in vivo*. Even though upregulation of MDR1 mRNA or protein is observed in imatinib-resistant CML patients, it will be necessary to measure intracellular imatinib levels to understand individual cases of imatinib resistance. Therefore, we ruled out a contribution from known mechanisms including P-gp, and postulated the involvement of a separate mechanism.

BCR-ABL has multiple downstream survival pathways, such as ERK1/2, ERK5, AKT, and JAK/STAT.^(14–17) We examined whether imatinib treatment inhibited these downstream factors and found that the phosphorylation of BCR-ABL, ERK5, AKT, and STAT5 was indeed downregulated in both K562/W and K562/R cells, whereas ERK1/2 was not inhibited by imatinib in K562/R cells (Fig. 2A,C). A similar result was obtained by treatment using BCR-ABL siRNA (Fig. 3B), which further indicated that ERK1/2 is phosphorylated by a BCR-ABL-independent mechanism in the K562/R cells. Next, the contribution of ERK1/2 to imatinib resistance in the K562/R cells was examined (Figs 4,5). Although the cells were not sensitive to treatment with 1 μM imatinib alone, co-administration with 1 μM U0126 inhibited ERK1/2 phosphorylation and dramatically induced K562/R cell death. U0126 is a known inhibitor of ERK5 as well,⁽³⁰⁾ but because imatinib inhibited ERK5 phosphorylation (Fig. 2C), most of the synergistic effect of U0126 was presumably mediated by its downregulation of ERK1/2, rather than ERK5. These results demonstrate that inhibition of not only BCR-ABL, but also ERK1/2, due to its activation being independent of the former, is necessary to overcome imatinib resistance in the K562/R cells.

Concerning ERK1/2 activation in K562/R cells, the factors responsible have not been determined. It is known, however, that U0126 inhibits ERK1/2 through MEK1/2, which may be directly upstream of ERK1/2 in this BCR-ABL-independent pathway. We have also shown that the aberrant activation of LYN or KRAS is not involved (Fig. 1B; Supporting Information Fig. S1). However, the possibility remains that unknown factors

could increase ERK1/2 sensitivity and activate this signal via weak activation of BCR-ABL.

Recently, new drugs have been developed to target the BCR-ABL-dependent and -independent imatinib-resistance mechanisms. Nilotinib and dasatinib have a greater affinity for BCR-ABL than imatinib, and inhibit BCR-ABL and Src kinase, respectively.^(31,32) U0126 co-treatment with dasatinib reverses LYN-dependent imatinib resistance,⁽³³⁾ suggesting the efficacy of its combination with molecular target drugs. Sorafenib, which inhibits multiple kinases, induces apoptosis in both BCR-ABL-expressing imatinib-sensitive and -resistant cells.^(34–36) It is possible that the combination of sorafenib with a BCR-ABL inhibitor works by inhibiting ERK1/2 activation in K562/R cells.

In conclusion, we demonstrate that ERK1/2, activated through a BCR-ABL-independent mechanism, contributes to imatinib resistance in certain CML cells (Supporting Information Fig. S3). Although further work is required to confirm whether or not this resistance mechanism occurs in patients with CML, our study shows that this mechanism can be overcome by inhibiting the ERK1/2 signaling pathway with specific drugs that could be candidates for targeting the CML cells resistant to imatinib.

Acknowledgments

This work was supported in part by a Grant-in-Aid for Scientific Research from the Japan Society for the Promotion of Science (JSPS) for Hideyuki Saito (KAKENHI 21390048) and Akinobu Hamada (KAKENHI 19590149) and from Cancer Research, Kiban Research, Houga Research from the Ministry of Education, Science, and Culture of Japan for Norie Araki (KAKENHI 17015034, 19390482, and 20659223, respectively). We thank Anthony Wilson, of the Tumor Genetics and Biology Department at Kumamoto University, for assistance with the English language presentation of this manuscript.

Disclosure Statement

None.

Abbreviations

ABL	Abelson
AKT	v-akt murine thymoma viral oncogene homolog
BCL	B-cell CLL/lymphoma 2
BCR	breakpoint cluster region
CML	chronic myeloid leukemia
CysA	cyclosporin A
LYN	v-yes-1 Yamaguchi sarcoma viral related oncogene homolog
P-gp	P-glycoprotein
PI3K	phosphoinositide 3-kinase
RAF	v-raf murine sarcoma viral oncogene homolog
RAS	rat sarcoma oncogene
STAT	signal transducer and activator of transcription

References

- 1 Kalidas M, Kantarjian H, Talpaz M. Chronic myelogenous leukemia. *JAMA* 2001; **286**: 895–8.
- 2 Capdeville R, Buchdunger E, Zimmermann J, Matter A. Glivec (STI571, imatinib), a rationally developed, targeted anticancer drug. *Nat Rev Drug Discov* 2002; **1**: 493–502.
- 3 Druker BJ, Guilhot F, O'Brien SG *et al*. Five-year follow-up of patients receiving imatinib for chronic myeloid leukemia. *N Engl J Med* 2006; **355**: 2408–17.
- 4 Daley GQ. Dodging the magic bullet: understanding imatinib resistance. *Cancer Biol Ther* 2003; **2**: 109–10.
- 5 Branford S, Rudzki Z, Walsh S *et al*. High frequency of point mutations clustered within the adenosine triphosphate-binding region of BCR/ABL in patients with chronic myeloid leukemia or Ph-positive acute lymphoblastic leukemia who develop imatinib (STI571) resistance. *Blood* 2002; **99**: 3472–5.
- 6 Roche-Lestienne C, Soenen-Cornu V, Grardel-Duflos N *et al*. Several types of mutations of the Abl gene can be found in chronic myeloid leukemia patients resistant to STI571, and they can pre-exist to the onset of treatment. *Blood* 2002; **100**: 1014–8.
- 7 Gorre ME, Mohammed M, Ellwood K *et al*. Clinical resistance to STI-571 cancer therapy caused by BCR–ABL gene mutation or amplification. *Science* 2001; **293**: 876–80.
- 8 Hamada A, Miyano H, Watanabe H, Saito H. Interaction of imatinib mesilate with human P-glycoprotein. *J Pharmacol Exp Ther* 2003; **307**: 824–8.
- 9 Hirayama C, Watanabe H, Nakashima R *et al*. Constitutive overexpression of P-glycoprotein, rather than breast cancer resistance protein or organic cation transporter 1, contributes to acquisition of imatinib-resistance in K562 cells. *Pharm Res* 2008; **25**: 827–35.
- 10 Mahon FX, Belloc F, Lagarde V *et al*. MDR1 gene overexpression confers resistance to imatinib mesylate in leukemia cell line models. *Blood* 2003; **101**: 2368–73.
- 11 Gambacorti-Passerini C, Barni R, le Coutre P *et al*. Role of alpha1 acid glycoprotein in the *in vivo* resistance of human BCR–ABL(+) leukemic cells to the abl inhibitor STI571. *J Natl Cancer Inst* 2000; **92**: 1641–50.
- 12 Donato NJ, Wu JY, Stapley J *et al*. BCR–ABL independence and LYN kinase overexpression in chronic myelogenous leukemia cells selected for resistance to STI571. *Blood* 2003; **101**: 690–8.
- 13 Dai Y, Rahmani M, Corey SJ, Dent P, Grant S. A Bcr/Abl-independent, Lyn-dependent form of imatinib mesylate (STI-571) resistance is associated with altered expression of Bcl-2. *J Biol Chem* 2004; **279**: 34227–39.
- 14 Jin A, Kurosu T, Tsuji K *et al*. BCR/ABL and IL-3 activate Rap1 to stimulate the B-Raf/MEK/Erk and Akt signaling pathways and to regulate proliferation, apoptosis, and adhesion. *Oncogene* 2006; **25**: 4332–40.
- 15 Sonoyama J, Matsumura I, Ezoe S *et al*. Functional cooperation among Ras, STAT5, and phosphatidylinositol 3-kinase is required for full oncogenic activities of BCR/ABL in K562 cells. *J Biol Chem* 2002; **277**: 8076–82.
- 16 Kirchner D, Duyster J, Ottmann O, Schmid RM, Bergmann L, Munzert G. Mechanisms of BCR–ABL-mediated NF-kappaB/Rel activation. *Exp Hematol* 2003; **31**: 504–11.
- 17 Buschbeck M, Hofbauer S, Di Croce L, Keri G, Ulrich A. Abl-kinase-sensitive levels of ERK5 and its intrinsic basal activity contribute to leukaemia cell survival. *EMBO Rep* 2005; **6**: 63–9.
- 18 Quintas-Cardama A, Cortes J. Molecular biology of BCR–ABL1-positive chronic myeloid leukemia. *Blood* 2009; **113**: 1619–30.
- 19 Pendergast AM, Quilliam LA, Cripe LD *et al*. BCR–ABL-induced oncogenesis is mediated by direct interaction with the SH2 domain of the GRB-2 adaptor protein. *Cell* 1993; **75**: 175–85.
- 20 McCubrey JA, Steelman LS, Abrams SL *et al*. Roles of the RAF/MEK/ERK and PI3K/PDEN/AKT pathways in malignant transformation and drug resistance. *Adv Enzyme Regul* 2006; **46**: 249–79.
- 21 Nishimoto S, Nishida E. MAPK signalling: ERK5 versus ERK1/2. *EMBO Rep* 2006; **7**: 782–6.
- 22 O'Brien J, Wilson I, Orton T, Pognan F. Investigation of the Alamar Blue (resazurin) fluorescent dye for the assessment of mammalian cell cytotoxicity. *Eur J Biochem* 2000; **267**: 5421–6.
- 23 Brauer KM, Werth D, von Schwarzenberg K *et al*. BCR–ABL activity is critical for the immunogenicity of chronic myelogenous leukemia cells. *Cancer Res* 2007; **67**: 5489–97.
- 24 Pao W, Wang TY, Riely GJ *et al*. KRAS mutations and primary resistance of lung adenocarcinomas to gefitinib or erlotinib. *PLoS Med* 2005; **2**: e17.
- 25 Agarwal A, Eide CA, Harlow A *et al*. An activating KRAS mutation in imatinib-resistant chronic myeloid leukemia. *Leukemia* 2008; **22**: 2269–72.
- 26 Bain J, McLauchlan H, Elliott M, Cohen P. The specificities of protein kinase inhibitors: an update. *Biochem J* 2003; **371**: 199–204.
- 27 Garnett MJ, Marais R. Guilty as charged: B-RAF is a human oncogene. *Cancer Cell* 2004; **6**: 313–9.
- 28 Weinstein-Oppenheimer CR, Henriquez-Roldan CF, Davis JM *et al*. Role of the Raf signal transduction cascade in the *in vitro* resistance to the anticancer drug doxorubicin. *Clin Cancer Res* 2001; **7**: 2898–907.
- 29 Davis JM, Navolanic PM, Weinstein-Oppenheimer CR *et al*. Raf-1 and Bcl-2 induce distinct and common pathways that contribute to breast cancer drug resistance. *Clin Cancer Res* 2003; **9**: 1161–70.
- 30 Kamakura S, Moriguchi T, Nishida E. Activation of the protein kinase ERK5/BMK1 by receptor tyrosine kinases. Identification and characterization of a signaling pathway to the nucleus. *J Biol Chem* 1999; **274**: 26563–71.
- 31 Kantarjian H, Giles F, Wunderle L *et al*. Nilotinib in imatinib-resistant CML and Philadelphia chromosome-positive ALL. *N Engl J Med* 2006; **354**: 2542–51.
- 32 Talpaz M, Shah NP, Kantarjian H *et al*. Dasatinib in imatinib-resistant Philadelphia chromosome-positive leukemias. *N Engl J Med* 2006; **354**: 2531–41.
- 33 Nguyen TK, Rahmani M, Harada H, Dent P, Grant S. MEK1/2 inhibitors sensitize Bcr/Abl+ human leukemia cells to the dual Abl/Src inhibitor BMS-354/825. *Blood* 2007; **109**: 4006–15.
- 34 Wilhelm SM, Carter C, Tang L *et al*. BAY 43-9006 exhibits broad spectrum oral antitumor activity and targets the RAF/MEK/ERK pathway and receptor tyrosine kinases involved in tumor progression and angiogenesis. *Cancer Res* 2004; **64**: 7099–109.
- 35 Rahmani M, Nguyen TK, Dent P, Grant S. The multitargeted inhibitor sorafenib induces apoptosis in highly imatinib mesylate-resistant bcr/abl+ human leukemia cells in association with signal transducer and activator of transcription 5 inhibition and myeloid cell leukemia-1 down-regulation. *Mol Pharmacol* 2007; **72**: 788–95.
- 36 Kurosu T, Ohki M, Wu N, Kagechika H, Miura O. Sorafenib induces apoptosis specifically in cells expressing BCR/ABL by inhibiting its kinase activity to activate the intrinsic mitochondrial pathway. *Cancer Res* 2009; **69**: 3927–36.

Supporting Information

Additional Supporting Information may be found in the online version of this article:

Fig. S1. Mutation analysis of KRAS in (A) K562/W and (B) K562/R cells. The T519C silent mutation was observed in both cell lines.

Fig. S2. (A) Expression of P-glycoprotein in crude membrane fractions of K562/W, K562/R, and prevK562/R cells. (B) Effects of imatinib treatment on the phosphorylation levels of ERK1/2 in K562/W, K562/R, and prevK562/R cells. Cells were treated with the indicated concentrations of imatinib for 24 h, and phosphorylation levels were analyzed by Western blotting.

Fig. S3. Scheme of a BCR–ABL-independent imatinib-resistant mechanism in K562/R cells. In K562/R cells, ERK1/2 is activated by a BCR–ABL-independent pathway. Imatinib inhibits BCR–ABL and decreases phosphorylated AKT, but not phosphorylated ERK1/2, which is activated by an unknown protein independent of BCR–ABL.

Please note: Wiley-Blackwell are not responsible for the content or functionality of any supporting materials supplied by the authors. Any queries (other than missing material) should be directed to the corresponding author for the article.

Suppression of galectin-3 expression enhances apoptosis and chemosensitivity in liver fluke-associated cholangiocarcinoma

Sopit Wongkham,^{1,4,6} Mutita Junking,^{1,4} Chaisiri Wongkham,^{1,4} Banchob Sripa,^{2,4} Siri Chur-in^{3,4} and Norie Araki^{5,6}

Departments of ¹Biochemistry, ²Pathology, ³Surgery, ⁴Liver Fluke and Cholangiocarcinoma Research Center, Faculty of Medicine, Khon Kaen University, Khon Kaen, Thailand; ⁵Department of Tumor Genetics and Biology, Graduate School of Medical Sciences, Kumamoto University, Kumamoto, Japan

(Received May 15, 2009/Revised July 12, 2009/Accepted July 20, 2009/Online publication September 1, 2009)

Cholangiocarcinoma (CCA) is a fatal disease with high resistance to anticancer drugs. This is probably in part due to enhanced resistance to apoptosis. We have previously shown that galectin-3 (Gal-3), a β -galactoside-binding lectin, is highly expressed in CCA tissues. In this study, we demonstrated further that Gal-3 plays a direct role in anti-apoptosis regardless of the apoptotic insults. The anti-apoptotic activity and chemoresistance of CCA cells were related to Gal-3 expression level. Suppression of Gal-3 expression with siRNA stimulated apoptosis. siGal-3-K626 transiently depleted Gal-3 expression to the baseline and dramatically induced apoptosis, while siGal-3-K402 suppressed Gal-3 expression by 50% and provoked cell apoptosis, but only under apoptotic insults (hypoxic conditions or short UV radiation). These actions were reversed in Gal-3 overexpressing CCA cells. The correlation between the degree of anti-apoptotic activity and the level of endogenous Gal-3 was demonstrated. Suppression of Gal-3 expression in CCA cells with siGal-3-K402 significantly enhanced apoptosis induced by cisplatin or 5-fluorouracil by approximately 10 times, whereas overexpression of Gal-3 led to an increased resistance to drugs. In summary, the present study showed that the cellular level of Gal-3 might contribute to the anti-apoptotic activity and chemoresistance of CCA cells. Hence, Gal-3 expression level in cancer cells or tissues may be a marker for predicting chemotherapeutic response, and Gal-3 may be a specific gene-targeting therapy option for treating CCA. (*Cancer Sci* 2009; 100: 2077–2084)

Cholangiocarcinoma (CCA), bile duct cancer, occurs with a varying frequency in different geographic regions of the world. It is rare in Western countries; however, in Khon Kaen, a province in the north-east of Thailand, the incidences of CCA in male and female residents are highest in the world.⁽¹⁾ The risk factor for CCA in this region has been shown to be the infection of liver fluke, *Opisthorchis viverrini*,⁽²⁾ whereas primary sclerosing cholangitis, hepatolithiasis, and choledochal cysts are risk factors for CCA in Western countries.

Cholangiocarcinoma (CCA) has traditionally resulted in a high mortality rate and poor prognosis. Although surgery is potentially curative in certain patients, failure has usually occurred due to recurrence. Adjuvant or neo-adjuvant therapy by chemotherapeutic drugs has been shown to improve local control, provide palliation, and prolong survival in various cancers; however, this is uncommon for CCA, owing to its poor response to therapy.⁽³⁾ Currently, adjuvant therapy, which enhances the cytotoxicity of chemotherapeutic drugs or sensitizes tumor cells to anticancer drugs, is showing encouraging results. This approach may increase the effectiveness of chemotherapy and improve prognosis in patients with CCA.

Recently, we have reported that all 53 CCA tissues expressed galectin 3 (Gal-3) regardless of histological type. A lower intensity was found in poorly differentiated CCA and was related to

lymphatic invasion.⁽⁴⁾ Even though there is substantial evidence regarding Gal-3 expression in various cancers, the significance of Gal-3 in the carcinogenesis and progression of CCA is yet to be determined.

Galectins are a family of proteins characterized by their affinity for β -galactoside, and the sequence similarities in the carbohydrate-recognition domain.⁽⁵⁾ To date, at least 15 galectin members have been identified and classified according to their structures into proto, chimera, and tandem-repeat types.⁽⁶⁾ Galectin-3 (Gal-3), a multifunctional protein, participates in a variety of biological events, for example cell adhesion, differentiation, proliferation, and apoptosis.^(5,7,8) Gal-3 has recently been shown to play a role in anti-apoptosis in several cell types.^(9–13) Peritoneal macrophages from Gal-3-deficient mice were more sensitive to apoptotic stimuli than those from control mice.⁽¹⁴⁾ Gal-3 could inhibit epithelial cell apoptosis induced by staurosporine, cisplatin, genistein, and anoikis.^(9–11,13) In addition, transfecting Gal-3 into epithelial cells provided them with resistance to apoptotic insult.^(9–13)

In this study, we examined the role of Gal-3 in anti-apoptosis in CCA cell lines by using RNA interference (RNAi) to knock-down endogenous Gal-3 expression. The possibility of using RNAi-mediated knockdown of Gal-3, in combination with a chemotherapeutic agent, is explored as a more effective treatment for CCA.

Materials and Methods

Cell culture. Four CCA cell lines were established from different histological grading of primary CCA tumors, KKU-OCA17 from a well-differentiated type, KKU-M055 and KKU-M214 from moderately differentiated types, and KKU-100 from a poorly differentiated type, as described by Sripa, *et al.*⁽¹⁵⁾ CCA cells were cultured in Ham's F-12 (Life Technologies, Rockville, MD, USA) supplemented with 10% fetal calf serum, 100 U/mL penicillin, and 100 μ g/mL streptomycin at 37°C and 5% CO₂.

Short interference RNA transfection. The coding sequence of the *Gal-3* gene in the human genome was submitted to Ambion siRNA Target Finder (http://www.ambion.com/techlib/misc/siRNA_finder.html). Two siRNAs specific for human galectin-3, siGal-3-K402 and siGal-3-K626, derived from the mRNA sequences beginning at nt 402 (5'-GGTGCCTCGCATGCTGTAAC-3') and nt 626 (5'-AAGTACTGGTTGAACCTGACC-3'), respectively, were purchased from JbioS (JbioS, Saitama, Japan). The lyophilized siRNAs were dissolved in annealing buffer, reheated to 95°C for 1 min, and incubated for 1 h at 37°C, by the protocol described previously.⁽¹⁶⁾ Transfection of both sequences was performed using Lipofectamine 2000

⁶To whom correspondence should be addressed.
E-mail: sopit@kku.ac.th, norie@gpo.kumamoto-u.ac.jp

(Invitrogen, Carlsbad, CA, USA) according to the manufacturer's instructions. CCA cells (8×10^4 cells in 2 mL complete culture medium) were seeded into a six-well plate for 24 h before transfection. The double-stranded siRNAs (100 pM) were transiently transfected into CCA cell lines K KU-100 and K KU-M214 using (2 μ g) Lipofectamine 2000 according to the manufacturer's instructions. After 4 h, the medium was changed to complete culture medium (Ham's F-12 with 10% fetal calf serum), and siRNA treated cells were used in the *in vitro* study within 48–72 h after transfection. As a control, cells were treated with siRNA-scramble (Ambion, Austin, TX, USA) or Lipofectamine 2000 under identical conditions.

Western blot analysis. Endogenous Gal-3 levels were determined using Western blotting. Before cell lysate preparation, apoptotic cells were washed out with PBS and then the adhered cells were extracted with lysis buffer (8 M Urea, 4% CHAPS) containing a complete protease inhibitor cocktail (Roche Molecular Biochemicals, Mannheim, Germany). The lysate was subjected to 12.5% SDS-polyacrylamide gel electrophoresis,⁽¹⁷⁾ and the protein expression of Gal-3 in CCA cells was determined by immunoblotting.⁽¹⁸⁾ Gal-3 was detected by 1:10 000 anti-Gal-3 antibody (Chemicon, Temecula, CA, USA), or 1:5000 anti- β -actin antibody (Sigma-Aldrich, St. Louis, MO, USA) as an internal control. The membrane was probed with horseradish peroxidase-conjugated antibody at 1:10 000 dilution (GE Healthcare, Buckinghamshire, UK). The immunoreactive proteins were visualized by Western Lightning Chemiluminescence Reagents (PerkinElmer, Boston, MA, USA). Quantitative analysis of Gal-3/ β -actin expression was performed using the Gel-Pro analyzer (Media Cybernetics, Silver Spring, MD, USA).

Time lapse assay. After 4 h of siRNA transfection, cells cultured in complete medium were placed under a time-lapse microscope and cultured further for 72 h, at 37°C and 5% CO₂. The images were obtained using an $\times 20$ UPlan Apo objective (Olympus, Tokyo, Japan). The camera, shutters, and filter wheel were controlled by MetaMorph imaging software (Universal Imaging, Dawningtown, PA, USA), and the images were collected at 5-min intervals for 48 h. Analysis was performed using MetaMorph software (Universal Imaging).

Construction of GFP Gal-3 expression vector. Human Gal3-inserted pET vector (Novagen, Madison, WI, USA) was a gift from Dr Ryuji Nagai (Department of Biochemistry, Kumamoto University School of Medicine, Kumamoto, Japan). DNA coding for Gal-3 was cut from the vector at the *EcoRI* site, followed by insertion into the multiple cloning site of the vector pEGFP-C1 (Clontech, Mountain View, CA, USA). The orientation of the construct was confirmed by digestion with *SmaI*, and the DNA sequence of the insertion was confirmed with a DNA sequencer (Applied Biosystems, Framingham, MA, USA). The plasmid was then transfected into K KU-M055 using Lipofectamine 2000 according to the manufacturer's instructions. After 24 h, the medium was changed to Medium G (Ham's F-12 medium containing 10% fetal calf serum and 0.6 mg/mL of G418 [Gibco, Carlsbad, CA, USA]). The cells were cultured in medium G for 2 weeks, and colonies resistant to G418 were screened by immunoblotting using the anti-Gal-3 antibody (Chemicon). Cells transfected with pEGFP-C1 vector without Gal-3 cDNA were used as a control.

Cell proliferation assay and drug treatment. After 24 h of siRNA transfection, cells were treated with various concentrations of cisplatin and 5-fluorouracil (5-FU) then incubated at 37°C, 5% CO₂ for another 48 h. The number of cells was determined using a sulforhodamine B assay (SRB; Sigma-Aldrich).⁽¹⁹⁾ Briefly, the culture medium was removed, and 10% cold trichloroacetic acid was added for 1 h at 4°C, and subsequently washed five times with deionized water. The plates were then air-dried and 0.4% SRB in 1% acetic acid was added for

30 min. Unbound dye was washed out five times with 1% acetic acid. After air-drying, SRB dye within cells were solubilized with 200 μ L of 10 mM Tris-base solution, and plates were shaken for at least 5 min. Absorbance was measured at 540 nm using a microplate reader (Tecan Austria, Salzburg, Austria).

Hypoxic conditions and UV irradiation. After 24 h of siRNA transfection, the cells were grown further at 37°C under hypoxic conditions (5% CO₂, 10% H₂, and 85% N₂) for 48 h, or exposed directly to UV radiation (250 mJoule/m²) for 4 s and then incubated at 37°C, 5% CO₂ for 48 h. The number of cells was determined using the sulforhodamine B assay.

Immunocytofluorescence staining. Cells were fixed in 4% paraformaldehyde for 15 min, permeabilized with 0.2% Triton X-100 for 5 min, and blocked with 1% bovine serum albumin in PBS for 1 h. Then, cells were incubated in 1:8000 of mouse monoclonal anti-Gal-3 antibody (Chemicon) for 1 h, then 1:1000 FITC goat antimouse IgG (BioSource, Camarillo, CA, USA) and 1:200 Hoechst 33342 (Molecular Probes, Eugene, OR, USA) for 1 h. The stained cells were observed using immunofluorescent microscope (Olympus).

Detection of apoptotic cells by flow cytometry using annexin V assay. After 24 h of siRNA transfection, cells were gently trypsinized and washed with ice-cold PBS. The cell pellet was resuspended in 100 μ L of Annexin-V-FLUOS labeling solution (Roche, Penzberg, Germany) and incubated at room temperature for 15 min. At least 20 000 cells were counted by flow cytometry (FACSCalibur flow cytometer) and data were analyzed using Cell Quest software (Becton Dickinson, San Jose, CA, USA).

Statistical analysis. Statistical analyses were performed using Sigma Stat version 3.1 software (Systat Software UK, London, UK). Results from flow cytometry, drug treatment, hypoxic condition, and UV irradiation are presented as mean \pm SD, and the significance of the differences were addressed by Student's *t*-test. A *P*-value of <0.05 was considered statistically significant.

Results

Suppression of Gal-3 induced apoptosis. To address the functional importance of Gal-3, we employed RNAi to transiently deplete the expression of Gal-3 in two CCA cell lines, K KU-100 and K KU-M214, which had high expression levels of Gal-3. Two siRNAs of 21-mer oligoribonucleotides targeting Gal-3, siGal-3-K402 and siGal-3-K626, were designed to suppress Gal-3 expression. The efficiency of the siGal-3s in suppression of endogenous Gal-3 is shown in Figure 1. As shown by Western blot analysis, transfection of K KU-100 CCA cells with siGal-3-K626 dramatically reduced Gal-3 protein >90% within 24 h, whereas cells transfected with siGal-3-K402 showed partial suppression of Gal-3 expression (~50%) (Fig. 1A). The efficiency of the siRNA was observed as early as 6 h after siGal-3 transfection and before apoptotic effect was observed (Fig. S1). Moreover, siGal-3 treatment effectively suppressed the level of Gal-3 in a time-dependent manner, and the suppression effects were detected until 72 h after transfection (Fig. 1B). Similar results were observed for K KU-M214 cells (data not shown). Neither siRNA-scramble, nor Lipofectamine 2000, affected the level of Gal-3 expression.

Within 24 h of siGal-3 treatment, apoptotic nuclei were readily observed in the cells treated with siGal-3-K626, but not in those treated with siGal-3-K402 or in control cells treated with Lipofectamine 2000 (Fig. 2A). To determine the anti-apoptotic activity of Gal-3, K KU-100 CCA cells transfected with siGal-3-K626 for 24 h were analyzed by flow cytometry using Annexin V and propidium iodide staining for early and late apoptotic cells. As shown in Figure 2(B), the number of Annexin V positive cells was much higher in K KU-100 cells treated with siGal-3-K626 compared to the control. Gal-3 suppressed